Metallomics

PAPER

View Article Online
View Journal | View Issue

Cite this: *Metallomics*, 2015, 7, 632

Synthesis of nickel–iron hydrogenase in *Cupriavidus metallidurans* is controlled by metal-dependent silencing and un-silencing of genomic islands†

Martin Herzberg, Marcel Schüttau, Matthias Reimers, Cornelia Große, Hans-Günther-Schlegel‡ and Dietrich H. Nies*

Received 14th November 2014,
Accepted 19th February 2015

DOI: 10.1039/c4mt00297k

www.rsc.org/metallomics

Cupriavidus metallidurans CH34 is able to grow autotrophically as a hydrogen-oxidizing bacterium and produces nickel-dependent hydrogenases, even under heterotrophic conditions. Loss of its two native plasmids resulted in inability of the resulting strain AE104 to synthesize the hydrogenases and to grow autotrophically in phosphate-poor, Tris-buffered mineral salts medium (TMM). Three of eleven previously identified catabolic genomic islands (CMGIs; Van Houdt *et al.*, 2009), two of which harbor the genes for the membrane-bound (CMGI-2) and the soluble hydrogenase (CMGI-3), were silenced in strain AE104 when cultivated in phosphate-poor TMM, explaining its inability to produce hydrogenases. Production of the soluble hydrogenase from the *aut* region 1 of CMGI-3, and concomitant autotrophic growth, was recovered when the gene for the zinc importer ZupT was deleted in strain AE104. The transcriptome of the Δ*zupT* mutant exhibited two up-regulated gene regions compared to its parent strain AE104. Expression of the genes in the *aut* region 1 increased independently of the presence of added zinc. A second gene region was expressed only under metal starvation conditions. This region encoded a TonB-dependent outer membrane protein, a putative metal chaperone plus paralogs of essential zinc-dependent proteins, indicating the presence of a zinc allocation pathway in *C. metallidurans*. Thus, expression of the genes for the soluble hydrogenase and the Calvin cycle enzymes on *aut* region 1 of CMGI-3 of *C. metallidurans* is under global control and needs efficient ZupT-dependent zinc allocation for a regulatory role, which might be discrimination of nickel.

Introduction

Currently, a picture is emerging as to how homeostasis of multiple transition metals in bacteria occurs.[1,2] Requirements include transport reactions, more specifically import and efflux across the inner and outer membrane,[3] a contribution from cellular thiols such as glutathione or bacillithiol,[4–6] changes in the metallation of metal-binding sites as a response to oxidative stress,[7] and the zinc repository, which has been recently identified in *Cupriavidus metallidurans*.[8] We selected nickel as a starting point to investigate the link between nickel and zinc allocation pathways in *C. metallidurans* because bacteria usually contain only a few nickel-dependent proteins.[9,10] Besides an urease, *C. metallidurans* possesses two [NiFe]-hydrogenases, a membrane-bound and a soluble, NAD^+-reducing enzyme, both of which are synthesized under autotrophic as well as heterotrophic growth conditions in the wild type strain CH34.[11] CH34 synthesizes neither a type 5 high-affinity hydrogenase[12] nor a sensory hydrogenase,[13] which is in alignment with the observation that the availability of molecular hydrogen is not required for synthesis of either hydrogenase.[11]

C. metallidurans is a betaproteobacterium able to maintain its transition metal homeostasis over a wide range of metal concentrations.[11,14,15] Metal import and export systems have been identified that interact in concert to establish a kinetic 'flow' equilibrium, which adjusts the concentration of the individual metal and the composition of all enzymes to meet the cellular requirements.[15–19] The most important and sophisticated metal-resistance systems of strain CH34 are encoded by two indigenous plasmids, pMOL28 and pMOL30.[11,14] These systems are absent in the plasmid-free strain AE104.[11]

Import of transition metal cations in *C. metallidurans* is achieved by a battery of highly redundant uptake systems,

Molecular Microbiology, Institute for Biology/Microbiology, Martin-Luther-University Halle-Wittenberg, Kurt-Mothes-Str. 3, 06120 Halle/Saale, Germany.
E-mail: d.nies@mikrobiologie.uni-halle.de; Fax: +49-(0)-345-5527010;
Tel: +49-(0)-345-5526352

† Electronic supplementary information (ESI) available. See DOI: 10.1039/c4mt00297k

‡ (1924–2013).

which have only minimal cation selectivity.[15] In addition to its role as a metal importer with low substrate specificity, the zinc importer ZupT of the ZIP protein family[20] is also essential for zinc supply under zinc starvation conditions, and even at higher zinc concentrations it is required for efficient allocation of the metal to zinc-dependent proteins[21] despite the fact that the other zinc uptake systems are still available to transport the metal into the cytoplasm.[15]

In the case of zinc ions, the zinc ion repository seems to counterbalance the transport processes. *C. metallidurans* contains at least 110 000 zinc-binding proteins per cell,[8] sometimes with more than one binding site per protein, but only 70 000 zinc atoms per cell when the metal is present at concentrations in the upper nM range. When μM concentrations (100–150 μM) of zinc are added, this number increases up to 120 000 atoms per cell, filling up the repository. Deletion of zinc efflux pumps (Δ*zntA* Δ*cadA* Δ*dmeF* Δ*fieF*) results in 250 000 zinc atoms per cell at 10 and 15 μM added zinc, and those cells are unable to grow at higher zinc concentrations. This indicates that efflux systems are needed to keep the number of zinc atoms at a level of 120 000 per cell, and that there is an overflow of the zinc repository at 250 000 atoms per cell or above, which subsequently leads to zinc toxicity.[8] Moreover, when *C. metallidurans* is treated with high concentrations of other transition metal cations, the resulting number of atoms per cell stayed in the range of 100 000 to 200 000,[15,21] indicating that the repository might also be involved in storage and sorting of these other ions, *e.g.* Ni(II).

A Δ*zupT* mutant contains only 20 000 zinc atoms when grown in the presence of zinc at a concentration in the upper nM range. The size of the zinc repository is not different between the mutant and its parent but an efficient zinc allocation, *e.g.* to the RpoC subunit of the RNA polymerase, was impaired in the Δ*zupT* mutant, even when it contained 120 000 zinc atoms at medium μM zinc concentrations.[8] Comparisons of the proteomes between mutant and parent did not yield any clues as to why the mutant had a problem with zinc allocation. Rather, the Δ*zupT* mutant up-regulated synthesis of a number of proteins important for chemolithoautotrophic growth, such as the soluble NAD-reducing hydrogenase and enzymes of the Calvin cycle. Synthesis of the hydrogenase is nickel-dependent, and is stimulated by carbon dioxide as electron sink during CO_2-fixation.[11] A defect in zinc allocation thus results in formation of a nickel-dependent protein, indicating an inter-connection between zinc and nickel homeostasis in *C. metallidurans*.

In this publication we demonstrate that the hydrogenases and Calvin cycle enzymes do indeed have the predicted functions and allow autotrophic growth of the Δ*zupT* mutant strain but not of its parent strain AE104 in phosphate-poor (642 μM phosphate) Tris-buffered mineral salts medium TMM. The genes encoding these proteins in CH34 are located on a genomic island, that was silenced in TMM-grown AE104 cells but which was 'un-silenced' again in the Δ*zupT* mutant. Unexpectedly, our approach also uncovered candidates for a zinc allocation pathway needed under conditions of severe zinc starvation. Together, these data indicate that *C. metallidurans* possesses ZupT-dependent zinc allocation pathways that "channel" the zinc repository to provide this metal efficiently to zinc-dependent proteins such as RpoC or maybe also HypA, which is crucial to discriminate nickel and to control further allocation of this metal to nickel-dependent proteins, such as hydrogenases.

Results

Autotrophic growth

A bottom-up proteomic approach revealed that the Δ*zupT* mutant up-regulated synthesis of the NAD^+-reducing hydrogenase and many Calvin-cycle enzymes when heterotrophically cultivated in phosphate-poor (642 μM phosphate) Tris-buffered mineral salts medium (TMM), while its parent strain AE104 did not,[8] although strain AE104 was capable of synthesizing hydrogenases in phosphate-rich (36 mM) growth medium.[11] To test if synthesis of these proteins had a physiological consequence, the *C. metallidurans* strains AE104, Δ*zupT* and, as a positive control the parental CH34 strain, were pre-cultivated heterotrophically to carbon exhaustion, diluted into fresh TMM with carbonate as sole carbon source, and cultivated with shaking at 30 °C under a "*Knallgas*" atmosphere.[11] Strain CH34 needed a lag phase of about 2 days to adapt to these conditions, and subsequently grew to 275 Klett units (KE) in the following 3 days (Fig. 1). The plasmid-free strain AE104, however, failed to grow within 8 days of incubation in TMM without an organic carbon source. The Δ*zupT* mutant of strain AE104 grew even more rapidly than CH34 but to a lower overall turbidity and with higher deviations between the individual cultures. This demonstrated that the Δ*zupT* strain with its up-regulated Calvin cycle and soluble hydrogenase proteins was indeed able to switch rapidly to autotrophic growth as a hydrogen-oxidizing bacterium.

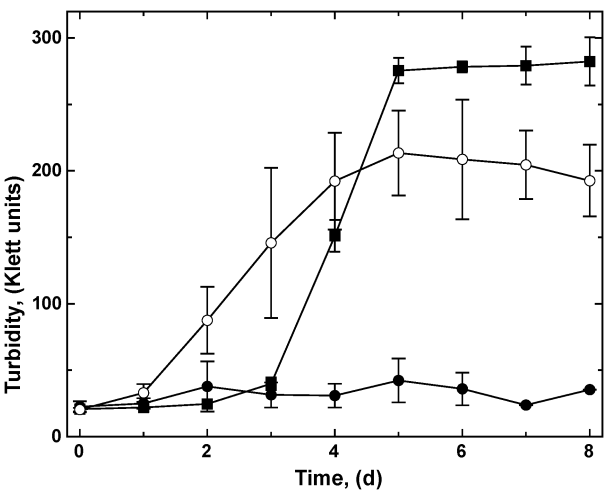

Fig. 1 Chemolithoautotrophic growth of *C. metallidurans* strains using molecular hydrogen, oxygen and carbon dioxide. Cells of *C. metallidurans* strain CH34 (pMOL28, pMOL30) wild type (filled squares, ■), its plasmid-free mutant AE104 (filled circles, ●) and the Δ*zupT* mutant of AE104 (open circles, ○) were cultivated in phosphate-poor TMM without an organic carbon source but under a gas atmosphere of $H_2 : O_2 : CO_2$ = 8 : 1 : 1 at 30 °C with shaking. Growth was monitored as Klett units. CH34 and AE104, three experiments, Δ*zupT* four experiments, deviation bars shown.

Characterization of the key enzymes needed for autotrophic growth

To confirm the identity and biochemical function of the key enzymes needed for autotrophic growth, crude extracts, soluble supernatant and membrane fractions from cells of the three strains CH34, AE104 and Δ*zupT* were separated on a non-denaturing polyacrylamide gel. Subsequently, an activity stain for hydrogenases was performed (Fig. 2). After autotrophic growth, extracts from strain CH34 exhibited activity of the membrane-bound hydrogenase while the corresponding activity band from the Δ*zupT* cells was significantly weaker. Strain AE104 did not grow autotrophically in phosphate-poor TMM (but heterotrophically as published[11]). After heterotrophic cultivation in TMM, only CH34 wild type showed activity of a membrane-bound hydrogenase (Fig. 2 bottom).

The specific activity of the soluble, NAD^+-reducing hydrogenase was determined as hydrogen-dependent NAD^+-reduction in crude extracts and soluble cell fractions (Table 1). After autotrophic growth in phosphate-poor TMM, hydrogenase activity above background was determined for strain CH34 and the Δ*zupT* mutant of strain AE104. After heterotrophic growth, significant hydrogenase activity could be measured for the Δ*zupT* mutant.

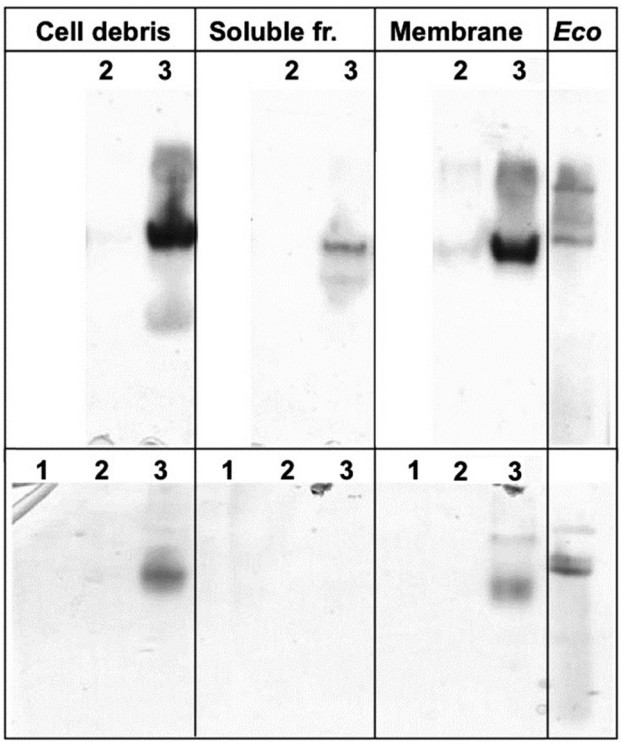

Fig. 2 Activity of membrane-bound hydrogenases. *C. metallidurans* strains were cultivated autotrophically (top) or heterotrophically (bottom) in phosphate-poor TMM, *E. coli* W3110 cells as control were grown heterotrophically in LB. Crude extracts of ultrasonicated cells, soluble and membrane fraction separated by ultracentrifugation were separated on a non-denaturing polyacrylamide gel in MOPS buffer pH 7 plus 4% (w/v) Triton X100, and an activity stain was performed as published.[22] *E. coli* crude extract (200 μg protein per lane) served as positive control. *C. metallidurans* strains were AE104 (1, no growth under autotrophic conditions in TMM), Δ*zupT* (2) or CH34 (3), each loaded at 50 μg protein per lane.

Table 1 Hydrogen-dependent NAD^+-reducing activity of *C. metallidurans* strains

		NAD^+-reduction rate, U g^{-1} protein	
Strain	Cultivation	Crude extract	Soluble fraction
CH34	Heterotrophically	1.1 ± 0.1	1.3 ± 0.6
AE104	Heterotrophically	1.2 ± 0.0	2.4 ± 2.6
Δ*zupT*	Heterotrophically	23.5 ± 19.2	58.8 ± 36.1
CH34	Autotrophically	16.0 ± 0.0	60.0 ± 0.0
AE104	Autotrophically	No growth	No growth
Δ*zupT*	Autotrophically	20.5 ± 0.0	10.9 ± 3.8

The four key enzymes for autotrophic growth, soluble and membrane-bound hydrogenase, ribulose-bisphosphate carboxylase and phosphoribulo-kinase, were purified from crude extract of *C. metallidurans* CH34 wild type cells. The specific activities and molecular masses confirmed that these proteins indeed performed the predicted functions (Table S1, ESI†), although the molecular masses of the hydrogenases were over- and that of the ribulose-bisphosphate carboxylase was under-estimated. The membrane-bound hydrogenase exhibited a K_m value of 38 μM for the artificial electron acceptor methylene blue in a 100% hydrogen atmosphere The procion dye HERD used for the last purification step competitively inhibited methylene blue reduction with a K_i of 4.1 μM (data not shown).

The kinetic mechanism of the NAD^+-reducing hydrogenase was analyzed in more detail using Hanes–Woolf plots as described by Segel.[23] The enzyme exhibited a typical ping-pong reaction mechanism with an apparent K_m for molecular hydrogen of 38 μM, NAD^+ of 242 μM and NADH (reverse reaction) of 60 μM (data not shown). In analogy to the protein from *Ralstonia eutropha* (synonym *Cupriavidus eutrophus*),[24,25] the enzyme from *C. metallidurans* was oxygen-tolerant and could be re-activated after oxygen treatment with NADH and molecular hydrogen (data not shown).

This demonstrated that deletion of the *zupT* gene for the zinc importer led to synthesis of the NAD^+-reducing hydrogenase and the Calvin cycle enzymes, which were fully functional, had the predicted biochemical functions, and enabled autotrophic growth.

Isolation of autotrophic mutants

It was unexpected that the plasmid-free strain AE104 failed to grow autotrophically in phosphate-poor (642 μM) TMM because it was able to grow in a phosphate-rich (36 mM) Schlegel–Gottschalk–Kaltwasser (SGK) medium.[11] Strain AE104 was treated with mutagenic agents (nitrite, EMS, NMG, mitomycin C) and mutants unable to grow autotrophically even in phosphate-rich SGK medium were isolated. A total of 16 mutants from 6400 colonies analyzed in two independent mutagenesis experiments were unable to grow autotrophically in SGK (7 from experiment 1, 9 from experiment 2; 3 nitrite-generated mutants, 5 EMS, 5 NMG, 3 mitomycin C, data not shown). A D-cycloserine selection procedure did not influence the number of successfully isolated mutant strains, and all mutagenic agents used generated mutants despite their different modes of action. Most of the mutant strains had a stable Aut^- phenotype and

did not generate revertants. Exceptions were one EMS mutant (spontaneous reversion rate 10^{-6}, reversion rate after a second EMS treatment 10^{-1}), and all mitomycin C mutants that reverted back to autotrophic growth with a spontaneous reversion rate of 10^{-2} (data not shown). In a control experiment with untreated cells, no mutants could be identified among 3200 tested colonies indicating that the mutants did not arise spontaneously.

Of the 16 mutants, 13 were unable to produce the soluble hydrogenase and the Calvin cycle enzymes, and 3 were additionally unable to synthesize the membrane-bound hydrogenase. Thus, absence of the native metal-resistance plasmids pMOL28 and pMOL30 in strain AE104 prevented autotrophic growth or synthesis of hydrogenases under heterotrophic conditions in phosphate-poor TMM but allowed both processes in phosphate-rich SGK medium. Treatment of strain AE104 with mutagenic compounds efficiently yielded pleiotropic mutants no longer able to synthesize the soluble hydrogenase and the Calvin cycle enzymes, even in phosphate-rich SGK-medium. A second or additional mutagenic event also prevented the synthesis of the membrane-bound hydrogenase. A metal and phosphate-dependent regulatory process is thus in control of hydrogenase gene expression in *C. metallidurans*.

Comparison of AE104 with CH34

To investigate the consequences of the plasmid loss on TMM-grown *C. metallidurans* cells, the transcriptome of the plasmid-free derivative AE104 was compared to that of parental strain CH34 (Table S2, ESI†). The cells were heterotrophically cultivated in phosphate-poor TMM without additions. To facilitate analysis of the data, a group of adjacent genes in the same direction of transcription that was not interrupted by other genes transcribed in the opposite orientation was designated as ''operon region'', and all operon regions in the *C. metallidurans* genome were numbered from Op0001f on chromosome 1 starting with Rmet_0001 to Op1929r on plasmid pMOL28, with ''f'' indicating the forward and ''r'' the reverse direction of transcription compared to the genome annotation[14] (data not shown). The *Q* values (ratios) AE104/CH34, sorted according to their protein products that were up- or down-regulated, are presented in Table S2 (ESI†). Only *Q* values were considered that were ≥ 2 or ≤ 0.5 with *D*-values (difference of the two data points divided by the sum of the standard deviations) >1 (Table S2, ESI†).

Only 11 genes were up-regulated (Table 2), four of which were in the divergently organized region Op1321r–Op1322f. These genes coded for the zinc-exporting P-type ATPase ZntA (Op1321r) and the 5′ end of a region $czcI_2C_2B_2'$ related to the *czcICBAD* resistance determinant on plasmid pMOL30; however, this region was interrupted by an inversion of a large part of chromosome 2 in the middle of the $czcB_2$ gene. Two genes in Op0335f encoded putative cytochrome *c* oxidase subunits of the respiratory chain, the others transposon-related proteins. Up-regulation of the Op1321r–Op1322f divergently oriented region indicated an impaired zinc homeostasis of strain AE104 when cultivated in TMM.

A total of 250 genes were down-regulated in strain AE104, most of them located in 6 gene regions (Fig. 3). Region 1 (*aut* region 1) from Op0421f to Op0431f contained 55 genes for the soluble, NAD^+-reducing hydrogenase and the Calvin cycle enzymes, region 3 had a total of 63 genes, including those for the membrane-bound hydrogenase (*aut* region 2) and degradation of aromatic carbohydrates.

Region 2 showed similarity to a catabolic genomic island.[26] Eleven catabolic genomic islands, CMGI-1 to CMGI-11, had been identified on chromosome 1 of *C. metallidurans*.[27] The regions 1 to 3, which were strongly down-regulated in strain AE104, were indeed identical with the predicted catabolic genomic islands CMGI-2 (= region 3 containing *aut* region 2), CMGI-3 (= *aut* region 1) and CMGI-4 (= region 2), respectively (Fig. 3). No CMGI had been identified on chromosome 2, so region 4 could not be matched in a similar way. With the exception of region 5 at the beginning of chromosome 1 and region 4 on chromosome 2, most of the genes down-regulated in AE104 compared to CH34 were located in CMGIs 1, 2, 3, 4. Expression of the *pitA* gene for the metal:phosphate importer and *pst* for the phosphate-specific ABC importer were not changed (data not shown).

Table 2 Comparison of the gene expression profiles of untreated CH34 wild type cells to AE104 cells[a]

Operon region	Name	Gene	*Q*	*D*	Description
Op1321r	Rmet_4594	*zntA*	**1.72**	2.88	Q1LEH0 heavy metal translocating P-type ATPase
Op1322f	Rmet_4595	*czcI2*	**2.03**	2.92	Q1LEG9 putative uncharacterized protein
Op1322f	Rmet_4596	*czcC2*	**23.34**	5.36	Q1LEG8 outer membrane efflux protein
Op1322f	Rmet_4597	*czcB2′*	**15.36**	9.68	Q1LEG7 secretion protein HlyD
Op0075f	Rmet_0260	—	**2.31**	2.48	Q1LRT0 putative transmembrane protein
Op0075f	Rmet_0261	*coxB*	**2.08**	2.49	Q1LRS9 cytochrome *c* oxidase subunit 2
Op0335f	Rmet_1171	*tnpA*	**7.03**	21.74	Q9F8S6 transposase (transposase, IS4 family)
Op0362r	Rmet_1251	*tnp*	*4.08*	0.61	Q1LNY9 putative uncharacterized protein
Op0663f	Rmet_2349	—	**2.44**	1.15	Q8GQ59 putative uncharacterized protein ORF C51
Op0671f	Rmet_2382	*tnpA*	**4.49**	23.38	Q1LB62 integrase, catalytic region
Op0934r	Rmet_3353	*tnpA*	**2.77**	4.55	Q9F8S6 transposase (transposase, IS4 family)

[a] Only the up-regulated genes are shown, while the complete gene-set is in the Table S2 (ESI). Genes in the same or adjacent operon regions are boxed. Provided are the *Q*-ratios AE104/CH34, bold-faced letters indicate significant differences, letters in italics not significant differences. The *D*-value is the distance of both mean values divided by the sum of both deviations. (If $D > 1$ the deviation bars do not touch or overlap) the data points are different with a probability in the *t*-test of $>95\%$.

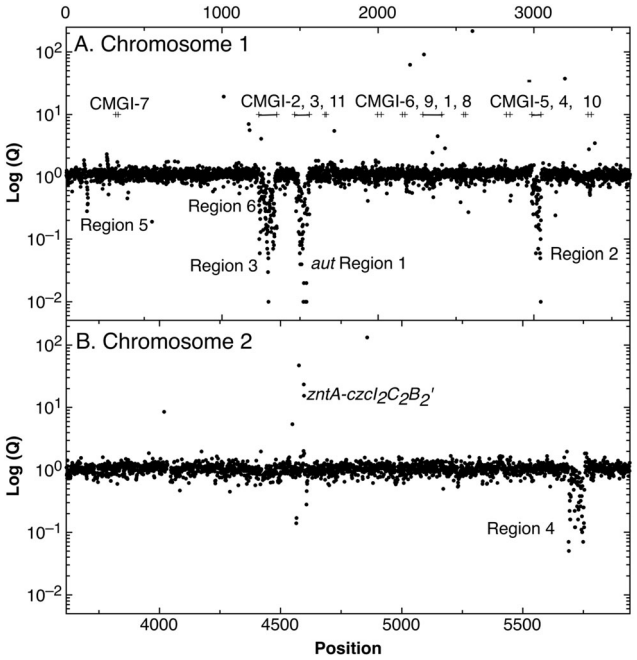

Fig. 3 Difference in gene expression between *C. metallidurans* parental strain CH34 and its plasmid-free derivative AE104. After cultivation of both strain in TMM without added metals, the cells were harvested, a gene array experiment performed and the ratios (*Q* values, closed circles) AE104/CH34 plotted against the position (Rmet number) on chromosome 1 (panel A) or chromosome 2 (panel B). Please note that the significance of the *Q* values is not indicated. The position of the *zntA-czcI*$_2$*C*$_2$*B*$_2$′ divergon and six large gene regions that were down-regulated in strain AE104 are indicated. The bars in panel A indicate proposed genomic islands on chromosome 1.[27]

When cultivated in phosphate-poor TMM, the plasmid-free strain AE104 exhibited silencing of some CMGIs including the *aut* region 1 as central part of CMGI-3 and *aut* region 2 on CMGI-2, activated recombination activity of four CMGIs, and increased the expression of the gene for the P_{IB1}-type zinc-exporting ATPase ZntA plus an adjacent inactivated paralogous region of the *czcICBA* metal resistance determinant on plasmid pMOL30. When grown instead in phosphate-rich SGK medium, gene products of this region could be found in AE104 cells but mutants could be readily isolated with these *aut* regions silenced even in phosphate-rich SGK medium. The metal and phosphate-dependent regulatory process in control of hydrogenase gene expression in *C. metallidurans* functioned by silencing the responsible *aut* regions located within CMGIs. The mutants indicated that both regions were silenced independently. Silencing required a increased cellular zinc availability, as demonstrated by the up-regulation of *zntA-czcI*$_2$*C*$_2$*B*$_2$′. Silencing occurred as a consequence of plasmid loss but only in the phosphate-poor TMM medium and not in the phosphate-rich, metal-complexing SGK medium.

Comparison of the proteome with the transcriptome

To analyze the connection between transcriptomic and proteomic results, the cellular content of a single protein in TMM-grown AE104 cells was compared with its gene expression signal measured by the gene array experiment. The luminescence of the single spots was normalized to a number of 10 000 gene-specific and intergenic RNAs. The overall data field resulting from this comparison resembled a triangle in the semi-logarithmical plot with the elongation factor TufA (Rmet_3324) on top of the triangle (Fig. S1, ESI†). Other proteins nearby were subunits of the ribosome (RpiL/Rmet_3335, RpsI/Rmet_0411, RplM/Rmet_0410, RpsU1/Rmet_2455, RpmL/Rmet_1162), the chaperone GroEL (Rmet_0616), alkyl hydroperoxidase Rmet_1950, and the extracytoplasmic solute-binding protein Rmet_0521, which is highly abundant in proteobacteria.[28]

The protein abundance was not a discrete function of the mRNA abundance measured as spot intensity in a gene array experiment. Nevertheless, the envelope curve that describes the increasing side of the triangle (Fig. S1, ESI†) suggested that a high cellular abundance of a given protein requires also a certain transcript level, as can be expected. On the other hand, a strong signal in the gene array experiment did not necessarily relate to an high protein abundance. This suggested a strong influence of translation control and protein stability on the protein copy-number, and that a protein copy number cannot be easily derived from transcriptomic data. A general lack of an mRNA–protein correlation has already been shown on the single-cell level[29] and was demonstrated here also on the population level. Nevertheless, absence of a signal in the gene array experiment should lead to a corresponding absence of the respective protein in the proteome, so that silencing of CMGIs was indeed the reason for the absence of hydrogenases and Calvin cycle proteins in AE104 cells grown in TMM.

Influence of 100 μM Zn(II) on the transcriptome of the plasmid-free strain AE104. To investigate the influence of an increased zinc availability on expression of the *aut* regions, a second transcriptome analysis compared AE104 cells incubated with or without 100 μM Zn(II). Three biological replicates were performed. The *Q* values (ratios), sorted into up- or down-regulated genes, are given in Table S3 (ESI†). Of 5850 genes, 5560 were not influenced, 153 were up-, and 137 were down-regulated. Only very few genes associated to CMGIs were changed in their expression but never the complete regions, *e.g.* 6 genes out of 116 of CMGI-2 were up-regulated between 2- and 3.9-fold, and one gene of the 96 gene region CMGI-3 (containing *aut* region 1) was up-regulated 2.3-fold. Increased zinc availability did not release the CMGIs from silencing in strain AE104.

Operon regions up-regulated at 100 μM Zn(II) were involved in iron–sulfur cluster biosynthesis, the phosphate starvation response, cadmium/zinc efflux by the P-type ATPases CadA and ZntA, and response to unfolded proteins in the periplasm (Table S3, ESI†). The interrupted *zntA-czcI*$_2$*C*$_2$*B*$_2$′ region was again up-regulated, indicating that the increased environmental zinc availability resulted in increased cellular zinc availability. Up-regulated zinc-containing proteins were fructose-bisphosphate aldolase, alcohol dehydrogenases and alkaline phosphatases. Down-regulated genes included those encoding TonB-dependent outer membrane proteins, several ABC transporters, periplasmic substrate-binding proteins, and di- and tricarboxylic acid transporters that might be involved in metal import. Two zinc-dependent

but B12-independent methionine synthases were also strongly down-regulated (0.06-fold, 0.17-fold; Table S3, ESI†). This all indicated an expected effect of a moderate zinc shock on AE104 cells: decreased import and increased export, repair of zinc-mediated damage to proteins and iron-dependent processes, and a shift in zinc-dependent proteins. But there was no influence on expression of the hydrogenase genes located in CMGI-2 and 3.

The *aut* region 1 was expressed in the Δ*zupT* mutant. Deletion of *zupT* disturbed zinc allocation even when sufficient zinc was available for the cells.[8,21] A third transcriptome analysis compared the transcriptomes of strain AE104 and its Δ*zupT* mutant. To address specifically zinc starvation conditions, both strains were cultivated in TMM in the presence of 50 μM EDTA to chelate Zn(II) and other metals, or in the presence of 10 μM Zn(II). Three biological replicates were done for each condition in strain AE104, two for each condition for the Δ*zupT* strain. The *Q* values (ratios) Δ*zupT*/AE104 under both conditions, sorted according to their protein products that were up- or down-regulated, are given in Table S4 (ESI†). *Q*(EDTA) was the ratio Δ*zupT*/AE104 in EDTA-grown cells, and *Q*(Zn) the ratios for cells grown in the presence of added zinc. Only *Q* values were considered that were ≥ 2 or ≤ 0.5 with *D*-values (difference of the two data points divided by the sum of the deviations) >1.

Eight genes were specifically up-regulated by zinc starvation in the Δ*zupT* mutant strain, *Q*(EDTA) $\geq$ 2 and *Q*(Zn) $\leq$ 0.5, seven of them significantly ($D > 1$). Six were all located in the same operon region Op0317f (Table 3). The region Op0318r adjacent to Op0317f contained the remaining gene (Rmet_1104, Table 3). The direction of transcription of the operon regions Op0317f and Op0318r was pointing towards each other and they were not divergently oriented. Regulation of expression of the genes in these regions was not due to a common promoter region but probably by the same regulator(s). The first of the 6 genes in Op0317f encoded CobW1, a putative metal chaperone, followed by 5 genes for paralogs of important zinc-dependent proteins. The single gene in Op0318r might encode a TonB-dependent outer membrane receptor. None of these proteins was found in the proteome of AE104 or Δ*zupT* cells grown without additions in mineral salts medium.[8] This region (*cobW1* cluster) might encode an outer membrane uptake system for zinc or zinc complexes, and the possible zinc chaperone CobW1, which might deliver Zn(II) specifically to the other five proteins under zinc starvation conditions.

The condition *Q*(EDTA) $\geq$ 2 and *Q*(Zn) $\geq$ 2, specifically up-regulated in the Δ*zupT* strain but independent of the two growth conditions, identified 21 genes in the operon regions Op0422r to Op0427f, which encode the enzymes of the Calvin cycle and those involved in formation of the soluble hydrogenase (Table 4) as *aut* region 1 of CMGI-2, confirming the proteomic, biochemical and physiological results. Two genes on Op1926f, which were transposon-associated (Table S4, ESI†) are also up-regulated.

A total of 654 genes were specifically down-regulated in the Δ*zupT* strain, *Q*(EDTA) $\leq$ 0.5 (Table S4, ESI†) and 345 genes had *Q*(EDTA) $\leq$ 0.5 and *Q*(Zn) $\leq$ 0.5. Among these were those for the sigma factor FliA and other proteins involved in cell motility, and as an artifact the Δ*zupT* gene, probably resulting from some transcripts coming from the deletion scar. Down-regulation of the genes for cell motility was also observed in the proteomic approach.[8] A total of 308 genes had *Q*(EDTA) $\leq$ 0.5 but *Q*(Zn) ratios that were not significantly changed. Among these were the gene for the zinc-exporting P-type ATPase ZntA and the metal-phosphate importer PitA, which is in agreement with the proteomic approach[8] (Table S4, ESI†).

If two additional *aut* region 1 genes (Rmet_1498, Rmet_1517) that were up-regulated only 1.7-fold by zinc are included, then the *cobW1* and *aut* region 1 genes were the only ones specifically up-regulated in the Δ*zupT* mutant strain compared to its parent strain. The *cobW1* cluster was repressed by zinc and might encode a specific zinc allocation pipeline to zinc-dependent proteins. The genes in *aut* cluster 1, in contrast, were not repressed by zinc.

The Δ*zupT* deletion in strain AE104 also influenced gene expression of catabolic metabolic islands CMGI-1, 10 and a few genes in CMGIs-2, 5, 7 (Table S4, ESI†), while loss of the plasmids resulted in down-regulation of CMGI-2, 3, 4. The expression pattern of the *aut* region 1 genes in CMGI-3 in the Δ*zupT* mutant compared to parent AE104 was unique: the genes at both ends of CMGI-3 were down-regulated similar to CMGI-1 and 10, while *aut* region 1 in the middle was strongly up-regulated in the Δ*zupT* mutant strain (Table 4 and Table S4, ESI†). This indicated that silencing of CMGI-3 as the result of plasmid loss was a process different from the regulatory event that specifically 'un-silenced' the *aut* region 1 on CMGI-3 but not *aut* region 2.

The number of proteins per cell, which were encoded by the genes in the CMGIs, was compared between the Δ*zupT* mutant cell and its parent AE104 (Table 5). For most CMGIs, gene expression was decreased in the Δ*zupT* mutant and consequently the number of proteins per cell was lower in the mutant. This was true even for CMGI-6, 8, 9, and 11 although no decreased gene expression had been observed here. This finding confirmed the transcriptomic data, because CMGI-3 encoded 11-times more protein in Δ*zupT* than in AE104

Table 3 The *cobW1* gene region[a]

Name	*Q*(Zn)	*Q*(EDTA)	Description
Op0317f			
Rmet_1098, CobW1	**0.48**	**17.91**	Cobalamin synthesis protein
Rmet_1099	**0.35**	**22.52**	GTP cyclohydrolase
Rmet_1100	**0.46**	**21.00**	Cysteinyl-tRNA synthetase
Rmet_1101	**0.49**	**14.38**	6-Pyruvoyl-tetrahydropterin synthase-like protein
Rmet_1102	**0.40**	**15.38**	Carbonic anhydrases
Rmet_1103	**0.49**	**13.61**	Q1LPD7 Dihydroorotase
Rmet_1104	**0.42**	**3.35**	TonB-dependent receptor

[a] None of the corresponding gene products was found in the proteome. The ratio of Δ*zupT*/AE104 in cells cultivated in the presence of 10 μM Zn, *Q*(Zn), or 50 μM EDTA, *Q*(EDTA) is shown. Values in bold-faced letters indicate significant changes ($\geq$2 fold, *D*-value $\geq$1). The genes are located in the operon region Op317f–Op318r and a similar regulatory pattern indicates that they might be present in operons.

Table 4 The cluster of genes for autotrophic metabolism (*aut* region 1 in CMGI-3) and its gene products[a]

	Proteins per cell		Transcriptome		
Name	AE104	Δ*zupT*	*Q*(Zn)	*Q*(EDTA)	Description
Op0422r					
Rmet_1497	NF	144 ± 10	0.93	1.44	Q1LN96 putative uncharacterized protein
Rmet_1498, CbbO	NF	169 ± 38	1.69	2.27	Q1LN95 rubisco activation protein
Rmet_1499, CbbQ	NF	433 ± 315	2.08	3.15	Q1LN94 ATPase associated with rubisco activation
Rmet_1500, CbbS	NF	1689 ± 1619	1.50	1.87	Q1LN93 ribulose bisphosphate carboxylase small chain
Rmet_1501, CbbL	*70*	6269 ± 139	1.64	1.78	Q1LN92 ribulose bisphosphate carboxylase large chain
Op0423f					
Rmet_1502, CbbR2	*NF*	*290*	4.28	3.05	Q1LN91 transcriptional regulator, LysR family
Rmet_1503, TnpA	NeF	NQ	0.44	1.41	Q9RBF5 insertion sequence IS*1090*
Op0424r					
Rmet_1504			0.59	1.22	Q1LN89 putative uncharacterized protein
Rmet_1505			*0.46*	1.64	Q1LN88 ISSod11, transposase
Rmet_1506, TnpA	NQ	NF	0.56	1.13	Q6SKD6 transposase
Rmet_1507, CbbF1	NeF	NeF	1.59	0.74	Q1LN86 D-fructose 1,6-bisphosphatase
Rmet_1508, CbbR2	NF	*47*	1.20	0.91	Q1LN85 transcriptional regulator, LysR family
Op0425f					
Rmet_1510, CbbE1	NF	*32*	1.76	0.95	Q1LN83 ribulose-5-phosphate 3-epimerase
Rmet_1511, CbbF2	*NF*	237 ± 200	4.16	2.61	Q1LN82 D-fructose 1,6-bisphosphatase
Rmet_1512, CbbT	NF	531 ± 23	1.20	1.06	Q1LN81 phosphoribulokinase
Rmet_1513, CbbT1	NF	327 ± 151	1.28	1.54	Q1LN80 transketolase
Rmet_1514, CbbZ1	*163*	120 ± 24	1.64	1.57	Q1LN79 phosphoglycolate phosphatase
Rmet_1515, CbbG1	62 ± 16	*573 ± 497*	1.39	1.22	Q1LN78 glyceraldehyde-3-phosphate dehydrogenase
Rmet_1516, Pgk1	277 ± 190	151 ± 28	pns	pns	Q1LN77 phosphoglycerat-kinase
Rmet_1517, CbbY	NF	*61*	1.66	2.51	Q1LN76 HAD-superfamily hydrolase subfamily IA, variant 3
Rmet_1518, CbbA2	68 ± 33	*191 ± 130*	1.62	1.72	Q1LN75 fructose-bisphosphate aldolase
Rmet_1519, PykA2	NeF	NeF	1.30	1.09	Q1LN74 pyruvate kinase
Rmet_1520, CbbJ1	NF	101 ± 13	1.70	1.18	Q1LN73 triosephosphate isomerase
Rmet_1521, CbbI1	NF	76 ± 14	3.22	2.87	Q1LN72 ribose-5-phosphate isomerase
Rmet_1522, HoxF	NF	1694 ± 1662	4.18	2.84	Q1LN71 NAD-reducing hydrogenase diaphorase moiety large subunit, 51 kDa subunit
Rmet_1523, HoxU	*NF*	1098 ± 989	6.99	5.85	Q1LN70 NAD-reducing hydrogenase diaphorase moiety small subunit
Rmet_1524, HoxY	*NF*	1855 ± 67	8.81	6.85	Q1LN69 NAD-reducing hydrogenase hoxS, 20 kDa delta subunit
Rmet_1525, HoxH	*34*	4611 ± 84	7.85	6.77	Q1LN68 nickel-dependent hydrogenase, large subunit
Rmet_1526, HoxW	NF	1766 ± 37	8.57	6.44	Q1LN67 HoxW, highly specific carboxyl-terminal protease involved in hydrogenase maturation
Rmet_1527, HoxI	NF	8605 ± 319	8.67	5.70	Q1LN66 cyclic nucleotide-binding domain (CNMP-BD) protein
Rmet_1528, PntAA′			4.17	2.38	Q1LN65 alanine dehydrogenase/PNT-like protein, interrpupted
Op0426r					
Rmet_1529	NF	373 ± 49	2.42	1.36	Q1LB62 integrase, catalytic region
Op0427f					
Rmet_1530, PntAA″			1.23	1.32	Q1LN63 alanine dehydrogenase/PNT-like protein, interrupted
Rmet_1531, PntAB			1.11	0.99	Q1LN62 pyridine nucleotide transhydrogenase subunit alpha, truncated
Rmet_1532, PntB	NeF	NeF	0.59	0.77	Q1LN61 NAD(P) transhydrogenase, beta subunit
Rmet_1533, HoxN	NeF	NeF	7.24	4.85	Q1LN60 high-affinity nickel-transporter
Rmet_1534, HoxV			11.16	4.92	Q1LN59 putative uncharacterized protein
Rmet_1535, HypA2	NF	622 ± 77	11.88	5.14	Q1LN58 hydrogenase nickel insertion protein HypA

Table 4 (*continued*)

	Proteins per cell		Transcriptome		
Name	AE104	Δ*zupT*	*Q*(Zn)	*Q*(EDTA)	Description
Rmet_1536, HypB2	NF	**5295 ± 249**	**10.59**	**5.67**	Q1LN57 hydrogenase accessory protein HypB
Rmet_1537, HypF2	NF	**504 ± 33**	**9.31**	**4.98**	Q1LN56 (NiFe) hydrogenase maturation protein HypF, carbamoyl phosphate phosphatase
Rmet_1538, HypC2	NeF	NeF	**8.36**	**4.24**	Q1LN55 hydrogenase assembly chaperone hypC/hupF
Rmet_1539, HypD2	NF	**493 ± 29**	**11.50**	**4.80**	Q1LN54 hydrogenase expression/formation protein HypD
Rmet_1540, HypE2	NF	**2965 ± 149**	**11.83**	**5.08**	Q1LN53 hydrogenase expression/formation protein HypE
Rmet_1541, HoxX	NF	**371 ± 61**	**10.76**	**4.83**	Q1LN52 formyl transferase-like protein
Rmet_1542, HoxA	***608 ± 41***	**240**	**10.37**	**4.64**	Q1LN51 hydrogenase transcriptional regulatory protein
Op428r					
Rmet_1543, CbbA	NF	NF	**2.11**	1.51	Q1LN50 stress responsive alpha-beta barrel, interruped
Op429f					
Rmet_1544					Q1LN49 transposase

[a] The protein numbers were taken from ref. 8. The transcriptome results were from Table S4 (ESI), and ratios Δ*zupT*/AE104 in zinc- or EDTA-treated cells are indicated. The proteins and genes were sorted according to the operon region (genes in the same orientation of transcription that are not interrupted by other genes in another orientation), from Op422r (r for reverse) to Op429f (f for forward). The region in chromosome 1 that contains these operon regions possesses three transposons or insertion elements in this region, which are marked by boxes. NF, not found in these two strains; NeF, never found in the proteome analysis done so far; NQ found but could not be quantified. Numbers in red indicate down-regulation, in green up-regulation, with bold numbers indicating significant differences. Up- and down-regulation in the proteome experiment was compared to strain CH34 (AE104 only) or to AE104 (Δ*zupT*) only.

Table 5 Comparison of the number of proteins encoded by catabolic metabolic genome islands in strain AE104 and its Δ*zupT* mutant strain[a]

Region	CMGI	AE104	Δ*zupT*	%
Rmet_0317–0333	CMGI-7	139 ± 10	235 ± 0	**169**
Rmet_1236–1351	CMGI-2	6961 ± 1310	3698 ± 713	53
Rmet_1465–1560	CMGI-3	3956 ± 1087	44 396 ± 7366	**1122**
Rmet_1660–1668	CMGI-11	1693 ± 0	0 ± 0	0
Rmet_1997–2020	CMGI-6	644 ± 47	164 ± 33	26
Rmet_2156–2172	CMGI-9	1306 ± 237	573 ± 118	44
Rmet_2287–2408	CMGI-1	3593 ± 874	2138 ± 339	60
Rmet_2549–2561	CMGI-8	178 ± 0	0 ± 0	0
Rmet_2824–2847	CMGI-5	1497 ± 296	1165 ± 143	78
Rmet_2987–3045	CMGI-4	1984 ± 143	1828 ± 135	92
Rmet_3347–3368	CMGI-10	1237 ± 711	534 ± 255	43

[a] Protein numbers taken from ref. 8, CMGI regions from ref. 27.

(Tables 4 and 5) due to increased synthesis of the *aut* region 1 gene products.

Importance of CobW1

To investigate the *cobW1* cluster in more detail, the *cobW1* gene for Rmet_1098/CobW1 was interrupted using a vector that inserted a *lacZ* gene with its own ribosome-binding site directly downstream of the interrupted gene. This mutation was introduced in the parent strain AE104 and its isogenic Δ*zupT* mutant. Metal resistance of the strains AE104, AE104(Δ*zupT*), AE104(Δ*cobW1::lacZ*) and AE104(Δ*zupT* Δ*cobW1::lacZ*) was compared in liquid culture (Fig. 4). The Δ*zupT*-strain showed a 3-fold decrease in cobalt and cadmium resistance and a slight decrease in zinc and EDTA resistance in liquid culture, as previously published.[15] Introduction of the Δ*cobW1::lacZ* mutation into strain AE104 lowered resistance to these substances

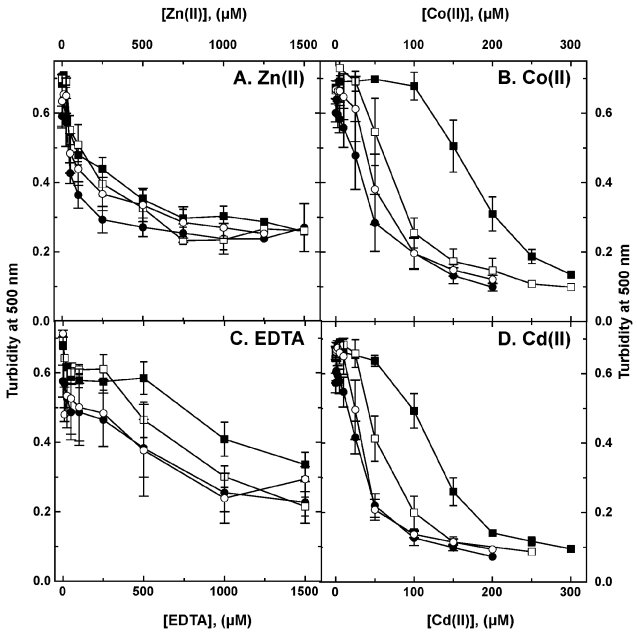

Fig. 4 Influence of deletions in the *zupT* and *cobW1* genes on metal and EDTA resistance. *C. metallidurans* strain AE104 (filled squares, ■) and its Δ*zupT* (filled circles, ●), Δ*cobW1::lacZ* (open squares, □) and Δ*zupT*Δ *cobW1::lacZ* (open circles, ○) mutant derivatives were cultivated for 20 h with shaking at 30 °C in TMM after 10-fold dilution in the presence of various metal and EDTA concentrations and the turbidity was determined as optical density at 500 nm.

significantly but not completely to the level of the Δ*zupT* mutant. Resistance of the Δ*zupT* Δ*cobW1::lacZ* double deletion strain, however, was very similar to that of the Δ*zupT* single

deletion strain (Fig. 4). This effect argued for a similar function of the uptake system ZupT and the putative zinc chaperone CobW1 in managing zinc starvation conditions and homeostasis of multiple metal ions.

As judged by the β-galactosidase fusion, expression of the *cobW1* gene was strongly up-regulated by metal starvation and down-regulated by metals in the Δ*zupT* background, leading to a 37-fold increase when comparing EDTA- and zinc-treated cells (Table 6). In the parent strain, expression levels of the *cobW1::lacZ* fusion were much lower, addition of zinc had no effect, and β-galactosidase activity in EDTA-treated cells was 20% of the value of the corresponding Δ*zupT* strain. These values were in full agreement with the gene array data (Table 3) and explained why CobW1 protein was not found in the proteome of (non-starving) Δ*zupT* mutant or AE104 parent strains.[8] The CobW1 system was only needed under conditions of severe metal starvation.

The *lacZ* reporter constructs all contained an integration of *lacZ* into the respective target gene, thereby interrupting it, so that the reporter strains were also all insertion mutants. To circumvent possible biases resulting from this situation and to exclude feedback effects, a *gfp* reporter plasmid was constructed and used to clone in front of *gfp* the 150 nucleotides upstream of *zupT* (*zupTp*) or *cobW1* (*cobW1p*). The resulting constructs were transferred by conjugation into various *C. metallidurans* strains, which were subsequently cultivated in TMM with or without added EDTA or zinc chloride (Table S5, ESI†). The basal level of the GFP-mediated fluorescence coming from those promoters was the specific fluorescence activity of TMM-grown cells divided by that from the negative control, the promoter-less *gfp* fusion. Subsequently, the specific fluorescence activities from the cultures with added EDTA or zinc were compared to these basal levels.

All regulatory events strictly depended on the presence of Zur/FurC, so that this protein was indeed required for regulation of *cobW1* expression in a similar fashion as previously shown for *zupT*. In the Δ*zur* mutant strain, *zupTp* and *cobW1p* expressed *gfp* at an increased high level of 7-fold and 5-fold compared to the negative control, respectively (Table S5, ESI†). Activity of the promoters was not different between strains CH34 and AE104 although the values coming from CH34 were slightly lower than those from AE104. Plasmid-borne genes were not required for these Zur-dependent regulatory processes but seem to ameliorate metal starvation mediated by EDTA to some extent. Deletion of the most important zinc efflux systems (strain Δe4 = Δ*zntA* Δ*cadA* Δ*dmeF* Δ*fieF*) did not influence the expression pattern but the additional deletion of *zupT* in Δe4 increased the basal level of expression while it decreased EDTA-dependent up-regulation. In AE104, activity of *zupTp* was at a high basal level (10-fold higher than the negative control), but it could be up-regulated 2-fold under extreme metal starvation conditions (10 mM EDTA). However, it was down-regulated 50% by addition of zinc. In contrast, the expression of the *cobW1p* promoter was at the level of the negative control in AE104, although it was also up-regulated by EDTA, and there was no difference between AE104 and its Δ*zupT* mutant. The *cobW1p* promoter was up-regulated by higher EDTA concentrations than the *zupTp* promoter (Table S5, ESI†).

The *cobW1* region was the only one specifically up-regulated in the Δ*zupT* strain under conditions of metal starvation and it was regulated mainly by zinc availability in a pattern reminiscent of the regulation of expression in Δ*zupT*; however, it was expressed more prominently during starvation. Moreover, Zur/FurC was essential for regulation of *cobW1p*, as it was observed for *zupTp*, Zur did not require ZupT-dependent zinc uptake and allocation for its function, and there seemed to be some feedback regulatory pathway that specifically up-regulates *zupT* expression in a Δ*zupT* mutant. Together, these data indicated that a specific zinc allocation pathway exists in *C. metallidurans* under conditions of severe zinc starvation. This pathway is composed of a TonB-dependent outer membrane protein, ZupT, and CobW1 that may "channel" the zinc repository to allocate zinc efficiently to paralogs of important zinc-dependent proteins, which are also encoded by genes of the *cobW1* cluster.

Table 6 Activity of a *cobW1::lacZ* reporter gene fusion[a]

	β-Galactosidase activity (U mg^{-1} d.w.)	
Additions	AE104(Δ*cobW1::lacZ*)	Δ*zupT* (Δ*cobW1::lacZ*)
None	1.20 ± 0.16	4.43 ± 1.05
10 μM Zn(II)	0.98 ± 0.15	3.12 ± 1.61
50 μM EDTA	24.3 ± 3.1	115 ± 20

[a] Derivatives of strains AE104 and Δ*zupT*, each containing a Δ*cobW1:lacZ* fusion, were cultivated in TMM to the late exponential phase of growth, diluted into fresh TMM to a turbidity of 30 Klett units and incubated with shaking at 30 °C until the turbidity has reached 60 KE. Subsequently, they were distributed into 96-well plates, the indicated compounds were added, incubation was continued for 3 h or for 16 h, and the specific β-galactosidase activity was determined.

Discussion

Global silencing of horizontally acquired genes

Three facts are important to explain the up-regulation of the *aut* region 1, which encodes the soluble hydrogenase and the Calvin cycle enzymes, in the Δ*zupT* mutant of the plasmid-free *C. metallidurans* derivative strain AE104 when cultivated in phosphate-poor Tris-buffered mineral salts medium TMM. First, *aut* region 1 is located in the middle of the catabolic genomic island CMGI-3.[27] Genomic islands are emerging as important factors for niche differentiation in bacteria[30–33] in a similar way to transposons and plasmids. Second, loss of the native plasmids pMOL28 and pMOL30 of the parental strain CH34 resulted in a silencing (or repression) of the CMGIs 2, 3, and 4, whereby CMGI-2 harbors the *aut* region 2 genes including those encoding the membrane-bound hydrogenase of *C. metallidurans*, while CMGI-4 harbors genes for catabolic enzymes not required for autotrophic growth. Third, in a unique fashion, expression of only the genes in *aut* region 1 were up-regulated, activated or 'un-silenced' (de-repressed) in the Δ*zupT* mutant of AE104, indicating a mechanism specific for *aut* region 1.

Silencing or repression of large gene regions can be accomplished on the DNA level by 'wrapping' these regions such that

access by RNA polymerase is hindered, or by influencing transcription by other means. Chromosome 1 of *C. metallidurans* contains 11 CMGIs, which could be the product of horizontal gene transfer and/or recombination events.[27] In *Escherichia coli*, the proteins HU and HN-S are important factors in genome organization, silence horizontally acquired genetic elements, and are both global transcription regulators. HU, present as homodimers $HupA_2$ and $HupB_2$ and as heterodimer HupAB depending on the growth conditions, re-organizes the transcriptome, binds non-coding RNAs, is involved in stress resistance, and is required for production of the stationary phase sigma factor RpoS.[34–38] Moreover, presence of polyphosphate stimulates degradation of HupA, which is linked to the exponential phase of growth and nucleoid organization,[39] linking growth phases and the phosphate status of the cell. Seven putative HupAB-related proteins are encoded by the *C. metallidurans* genome, three on the plasmids (Rmet_6397, 6191, 6090) and four on the chromosomes (Rmet_3538, 4749, 4742 and 5558). These 4 proteins could be found in the proteome of *C. metallidurans* with copy-numbers of about 6000, 6000, 8500 and 1700 per cell, respectively, which is maintained between CH34, AE104 and Δ*zupT*.[8] These numbers were 10-fold lower than those determined for *E. coli*,[40] perhaps due to the different methods used.

H-NS silences foreign DNA[41] by wrapping the DNA.[42] The proteins with the highest similarity to *E. coli* H-NS are Rmet_3677 with about 3800 copies per cell and the more distantly related Rmet_5562 with about 450 copies per cell. Both did not change their numbers between CH34, AE104 and Δ*zupT*[8] but the gene for Rmet_3677 was up-regulated 2.5-fold in AE104 cells treated with 100 μM Zn(II) (Table S3, ESI†), clearly indicating the influence of zinc on H-NS in *C. metallidurans*.

Sigma factors and metal homeostasis

The activity of the RNA polymerase in the global control of transcription initiation can be influenced by sigma factors or activators while repressors usually act upon one or a few operons only. *C. metallidurans* contains 11 sigma factors of the extracytoplasmic function (ECF) family,[43–46] arranged in four groups of related proteins. *C. metallidurans* often contains between two and four paralogs of these proteins, which substitute each other in deletion strains, *e.g.* the zinc-exporting P-type ATPases ZntA, CadA, PbrA and CzcP.[17,47] To characterize the contribution of these ECF sigma factors to metal resistance we therefore produced double or triple deletion mutants of *C. metallidurans* CH34 in which all genes encoding related ECF sigma factors were deleted. These mutants were tested for the impact of these deletions on the cellular metal content, the transcriptome, and the ability of the respective strain to handle a metal mixture composed of 30 μM each of $CoCl_2$, $NiCl_2$, $CuCl_2$, $ZnCl_2$ and $CdCl_2$ (C. Große and D. H. Nies, unpublished). *C. metallidurans* CH34 is able to deal with all of these metals in parallel,[15] however, treatment with this metal mixture resulted in down-regulation of *aut* region 2 on CMGI-2 and *aut* region 1 on CMGI-3 but not of CMGI-4, indicating that the CMGIs 2 and 3 are indeed silenced under conditions of metal stress. Deletion of groups of sigma factors had no effect except in the triple deletion strain CH34 (Δ*rpoEP cnrH::pLO2-lacZ*). This strain contained a significantly higher nickel content and expressed the *aut* region 1 similar to AE104Δ*zupT* (C. Große and D. H. Nies, unpublished). CnrH is the sigma factor required for expression of the *cnrCBA* nickel resistance determinant on plasmid pMOL28,[48–50] which explains the higher nickel content of the cells. So, when the metal content of *C. metallidurans* was increased, CMGIs were silenced, but when specifically the nickel content was increased even more, *aut* region 1 was un-silenced again. Un-silencing of this region is prevented by an efficient zinc allocation but is facilitated by nickel.

These results demonstrated that a perturbed metal ion homeostasis was probably responsible for silencing of CMGI-2, -3, and -5 in strain AE104, CMGI-1 and -11 in the isogenic Δ*zupT* mutant, and CMGI-2 and -3 in metal mixture-treated CH34 cells. Interestingly, such a link between metal homeostasis and hydrogenase synthesis has also been shown for *E. coli*.[51] Up-regulation of the *zntA-czcI*$_2$*C*$_2$*B*$_2$′ region on chromosome 2 is also in agreement with a disturbed metal homeostasis or increased zinc availability in TMM-grown AE104 cells. Moreover, strain AE104 readily produced hydrogenases and was able to grow autotrophically in phosphate-rich SGK mineral salts medium;[11] however, this ability was easily lost again in AE104 mutants.

Zinc speciation in the growth medium and zinc uptake

The phosphate-poor TMM[11] contains 642 μM phosphate, 1 mM magnesium chloride, 200 μM calcium chloride, 5 μM iron ammonium citrate and nM concentrations of the other essential transition metal cations, *e.g.* 200 nM zinc.[8,21] Calculated from the solubility constants of the respective metal phosphate compounds, which are in the in the region of 10^{-30} to 10^{-40} for the transition metal cations and Ca(II), and 10^{-25} for Mg(II),[52] most of the transition metal cations and also Ca(II) should reside in disperse metal phosphate precipitates, with magnesium filling up the remaining phosphate ions. The "free" Zn(II) concentrations under these conditions is calculated from the solubility constant to be 16.3 pM. The other anions, such as hydroxide, carbonate, sulfate, and the Tris buffer possess much lower solubility constant than phosphate, are thus not able to compete with phosphate for these cations, and do not need to be considered to understand the speciation of divalent metal cations in the growth media used.

In phosphate-rich SGK,[53] the phosphate concentration of 36 mM is much higher than that of the metal cations, so that only 3.3% of the phosphate pool in the growth medium should harbor a metal cation. The remaining 96.7% of the phosphate should be HPO_4^{2-} and $H_2PO_4^-$ at neutral pH values. In this medium, the "free" Zn(II) concentration is calculated to be only 1.12 pM.

Uptake of Zn(II) and the other transition metal cations (iron not considered here) is by ZupT and PitA. Since a Δ*zupT* Δ*pitA* double mutant is still able to import zinc, at least one more metal cation importer is involved, *e.g.* one of the three CorAs.[15] The ability of ZupT to fetch zinc ions at low concentrations can be judged by the decreased EDTA resistance of the Δ*zupT* mutant on solid TMM medium. The MIC value is 300 μM compared to 1.5 mM of strain AE104.[15] Using the stability constant of zinc

EDTA complexes,[54] the "free" zinc concentration at 300 μM EDTA and 200 nM Zn(II) is 53 aM. So, ZupT is needed to gather Zn(II) at "free" concentrations of 50 aM and below, which is sufficient to access the "free" zinc concentration in the phosphate-containing TMM and SGK media.

The PitA protein imports metal:phosphate complexes in *C. metallidurans*[15] and other prokaryotes.[55,56] As judged by the activity of the *lacZ* reporter gene fusion[15] PitA is the most strongly expressed metal uptake system in *C. metallidurans*. In SGK with most of the phosphate anions not bound to metal cations, PitA should mainly import just phosphate and only very few metal:phosphate complexes, resulting in a low PitA-mediated influx rate of metals. In contrast, in phosphate-poor TMM, with all phosphate ions bound to metal cations, PitA should import much more metal:phosphate complexes into the cell. In *C. metallidurans* CH34 wild type, the Czc system encoded on plasmid pMOL30 interferes with a too extensive zinc accumulation by CzcP- and CzcD-mediated export from the cytoplasm to the periplasm, and from here by the CzcCBA transenvelope efflux complex further on to the outside.[17] CzcP and CzcD export rapidly loosely bound zinc while the P-type APTases ZntA and CadA more tightly bound zinc, albeit with a lower export rate.[17] Assuming that phosphate-bound zinc could represent loosely bound zinc and zinc bound within the zinc repository or to thiols more tightly bound zinc, the products of the Czc system would be the antagonists of PitA in phosphate-poor environments and remove surplus transition metals from phosphate complexes in the cytoplasm and periplasm.

Consequently, the plasmid-free and Czc-free strain AE104 is not able to counterbalance the increased influx of zinc by the PitA system in TMM, leading to the observed mild zinc stress in these cells as indicated by the up-regulation of *zntA* and $czcI_2C_2B_2'$. In contrast, PitA imports not so many metal:phosphate complexes when strain AE104 grows in SGK, and there is consequently no need for *czc*-mediated zinc efflux. The resulting mild zinc stress is responsible for the specific silencing of the CMGIs specifically in TMM-grown AE104 cells, and also in metal-shocked CH34 cells as outlined above.

Expression of *pitA* is up-regulated with increasing phosphate content of the growth medium (up to 4 mM phosphate) but is down-regulated again at higher phosphate concentrations, except in the Δ*zupT* deletion strain.[15] This indicates that expression of *pitA* is influenced by zinc availability rather than by phosphate. Indeed, addition of zinc led to down-regulation of the *pitA-lacZ* reporter but this process did not require the Zur (FurC) zinc uptake regulator in *C. metallidurans*,[57] indicating the presence of additional zinc-dependent regulatory pathways in this bacterium. This pathway is also responsible for zinc-dependent down-regulation of other metal uptake systems such as $CorA_1$, $CorA_2$, $CorA_3$ (ref. 57) and may have a global regulatory function, which might also include silencing of CMGIs.

The Zur regulon

Zur (previously FurC) is required for control of expression of *zupT*.[57] Besides expression of the genes of the *aut* region 1 on CMGI-3, which were up-regulated independent of zinc availability (Table 4), the only genes up-regulated in the Δ*zupT* mutant under metal starvation conditions were those in the adjacent operon regions Op0371f and Op0318r (Table 3). Op0318r contains the gene for a TonB-dependent outer membrane protein Rmet_1104, which could catalyze the transport of zinc compounds across the outer membrane as in the cyanobacterium *Anabaena* sp.[58] The preceding operon region Op0371f comprises 6 genes in the same direction of transcription, which might be a hexacistronic operon. Rmet_1103 is a dihydroorotase, Rmet_1102 a carbonic anhydrase, Rmet_1101 a 6-pyrovoyl-tetrahydropterin synthase, Rmet_1100 a cysteinyl-tRNA synthetase and Rmet_1099 a GTP cyclohydrolase (Table 3), all are zinc-dependent proteins[59–62] with paralogs encoded in other parts of the genome. In the case of the cysteinyl-tRNA synthetase, the zinc ion is essential to discriminate between the related amino acids cysteine and serine[63] and the metal has a similar importance for the other proteins.

The first gene of the putative operon in region Op0317f encodes Rmet_1098 or CobW1, a homolog of YeiR from *E. coli*,[64] which is a zinc-binding metal chaperone and GTPase. Deletion of the respective gene from *E. coli* leads to sensitivity to EDTA or cadmium caused by zinc depletion.[64] When *cobW1* was interrupted by a *lacZ* insertion, the resulting strain displayed a similar EDTA and metal resistance as the Δ*zupT* strain, and the phenotype of the double mutant was similar to that of the single mutants, and to that of Δ*yeiR* in *E. coli*. As judged by the reporter activity, *cobW1* was up-regulated by zinc starvation in strain AE104 but more strongly so in the Δ*zupT* strain. CobW1 and YeiR belong to the COG0523 subfamily of G3E-GTPases, and the other three families of the G3E family of GTPases are represented by HypB, UreG and MeaB, which insert nickel or cobalt ions into hydrogenases, ureases or methylmalonyl-CoA mutases, respectively.[64] CobW1 might insert zinc into the proteins encoded downstream of *cobW1*, and the similar phenotype of the *cobW1* insertion mutant and the Δ*zupT* deletion mutant indicates that the Zn(II) ion might originate from ZupT. CobW1 might therefore "channel" the cytoplasmic zinc repository in *C. metallidurans* to provide the metal rapidly to zinc-requiring proteins under zinc starvation conditions.

Similar operon regions, all containing the gene for a CobW-like protein and paralogs of zinc-requiring proteins, exist in other bacteria of the *Burkholderiales*.[65] In *C. metallidurans*, the strong influence of metal starvation (Table 3) and a predicted Zur-binding site upstream of the operon region[65] indicates that Op0317f is likely a Zur-dependent operon, although binding of Zur to this site remains to be demonstrated. Zur bound to the predicted site upstream of *zupT*[67] and another Zur-binding site is located upstream of the *zur* gene. The *zur* gene itself (Rmet_0128, *furC*) is the first gene of operon region Op0032r and has a predicted Zur-binding site upstream in the regulatory region. The *zur* gene is followed by two genes for additional members of the COG0523 protein family, $cobW_2$ (Rmet_0127) and $cobW_3$ (Rmet_0125), which contains another Zur-box upstream, an uncharacterized protein (Rmet_0124), a TonB-dependent outer membrane protein (Rmet_0123), and, between the *cobW* genes, a *dksA* gene (Rmet_0126). While the TonB-dependent outer

membrane and the uncharacterized protein were not found in the proteome of *C. metallidurans*, CobW2 was present in about 2000 copies per cell, CobW3 in 300, the DksA protein in 3000 and Zur in 100 copies per cell. These numbers did not change when *zupT* was deleted.[8] These are all no longer putative proteins and are all clearly required for growth under mild zinc starvation conditions in TMM.

DksA

DksA is a global regulator in *E. coli* that interacts with ppGpp as cofactor, binds through a zinc-finger motif to the RNA polymerase, altering the kinetics of transcription initiation.[66] *C. metallidurans* has three genes for DksA paralogs in addition to Rmet_0126, Rmet_4453, 4470, and 4602 on chromosome 2. Although the Rmet_0126 DksA is present in a high copy number in the cell, the other three paralogs were not found in the proteome.[8] Nevertheless, expression of Rmet_4602 was down-regulated in Δ*zupT* compared to AE104 when cultivated in the presence of EDTA. The three putative DksA paralogs Rmet_4453, 4470, and 4602 contained two pairs of conserved cysteine residues that are involved in formation of the zinc-finger motif (CcXCh–X_{16}–CX_2C).[67,68] In contrast, the Rmet_0126 DksA has three of these cysteine residues changed to threonine, serine or alanine, respectively (CX_2T–X_{16}–SX_2A). As the copy number of the Rmet_0126 DksA approaches the number of RNA polymerase molecules in the cell, this protein might link the status of the overall transition metal homeostasis with the upper levels of the cellular hierarchical control mechanisms.

Experimental

Bacterial strains and growth conditions

Strains used for experiments were derivatives of the strain AE104, a megaplasmid-free derivative of *C. metallidurans* CH34[11] and its Δ*zupT* deletion mutant.[15] Tris-buffered mineral salts medium[11] containing 2 g sodium gluconate per L (TMM) was used to cultivate these strains aerobically with shaking at 30 °C. Analytical grade salts of heavy metal chlorides were used to prepare 1 M stock solutions, which were sterilized by filtration. Solid Tris-buffered media contained 20 g agar per L.

Autotrophic growth in TMM was performed in serum bottles with a "*Knallgas*" atmosphere of 80% H_2, 10% CO_2, and 10% O_2 in 90% of the total volume of the bottle. The remaining 10% was filled with the growth medium. The pre-culture was cultivated heterotrophically in TMM on gluconate to carbon exhaustion and subsequently diluted 100-fold with TMM without gluconate for the autotrophic culture.

For autotrophic growth in phosphate-buffered mineral salts medium (SGK),[53] the gas atmosphere also contained a mixture of H_2, O_2, and CO_2 (8 : 1 : 1, vol/vol/vol). Growth rates were determined by optical density measurements of suspensions growing in 300 mL Erlenmeyer flasks, which were shaken in a water bath at 30 °C. For the heterotrophic de-repression of the four key enzymes of the autotrophic metabolism IND medium was used. This medium contained per 1 L: 9.0 g $Na_2HPO_4{\cdot}12H_2O$; 1.5 g KH_2PO_4; 3.0 g NH_4Cl; 0.2 g $MgSO_4{\cdot}7H_2O$; 0.02 g $CaCl_2{\cdot}2H_2O$; 36 mg iron-ammonium-citrate; 0.1 mL SL6 according to Pfennig 10-fold concentrated;[69] 18 μg $Na_2MoO_4{\cdot}2H_2O$; 42 μg $MnCl_2{\cdot}4H_2O$; 140 μg $ZnSO_4{\cdot}7H_2O$; 3 g glycerol and 9 g sodium gluconate. The pH value was adjusted to 6.9 ± 0.1.

For enzyme purification cells were cultivated in a 10 L fermentor (Biostat, Braun, Melsungen, Germany) at 30 °C, 600 rpm and a gas flow of 500 mL min^{-1}. Cultures grown in IND medium were sparged with air, and cultures of autotrophically growing cells with a mixture of 80% H_2, 10% O_2 and 10% CO_2. Both media additionally contained 2 mL per 8 L polypropylenglycol P200, 20% in 96% ethanol to prevent foam formation. The cells were harvested at the end of the exponential growth phase, washed with KP50 (50 mM potassium phosphate buffer, pH 7.0, containing 10 mM $MgCl_2$) and stored at −20 °C.

Dose–response growth curves in 96-well plates

Growth curves for *C. metallidurans* were conducted in TMM. A pre-culture was incubated at 30 °C, 250 rpm up to early stationary phase, then diluted 1 : 20 in fresh medium and incubated for 24 h at 30 °C and 250 rpm. Overnight cultures were used to inoculate (at a ratio of 1 : 10) parallel cultures with increasing metal or EDTA concentrations in 96-well plates (Greiner). Cells were cultivated for 20 h at 30 °C and 1300 rpm in a neoLab Shaker DTS-2 (neoLab, Heidelberg, Germany) and the optical density was determined at 600 nm as indicated in a TECAN infinite 200 PRO reader (TECAN, Männersdorf, Switzerland). To calculate the IC_{50} value (metal concentration that led to turbidity reduction by half) and the corresponding *b*-value (measure of the slope of the sigmoidal dose–response curve), the data were adapted to the formula $OD(c) = OD0/\{1 + \exp((c - IC50)/b)\}$, which is a simplified version of a Hill-type equation as introduced by Pace and Scholtz[70] as published.[71] $OD(c)$ is the turbidity at a given metal concentration, OD0 is the turbidity with no added metal and *c* the metal concentration.

β-Galactosidase assay and *lacZ*-reporter constructions

C. metallidurans cells with a *lacZ* reporter gene fusion were cultivated as a pre-culture in TMM containing 1.5 mg L^{-1} kanamycin at 30 °C, 250 rpm for 30 h, then diluted into fresh medium to a density of 30 Klett units and incubated at 30 °C. At a cell density of 60 to 70 Klett units, metal salts were added in different concentrations and cells were incubated with shaking for a further 3 h and harvested by centrifugation (30 min at 5000 rpm). The specific β-galactosidase activity was determined in permeabilized cells as previously published with 1 U defined as the activity forming 1 nmol of *o*-nitrophenol min^{-1} at 30 °C.[72] The *lacZ* reporter gene was inserted into the target gene (Rmet_1098) to construct reporter operon fusions. This was done by single cross-over recombination in *C. metallidurans* strains. A 300–400 bp PCR-product of the central region of the genes (Rmet_1098/$cobW_1$) were amplified from total DNA of strain CH34 (primer: Rmet_1098 PstI Dis – AAACTGCAGGGCCGC AGTCTCAATGAGG & Rmet_1098 XbaI Dis – AAATCTAGAG GGCGCTTTCGATGCTTCC) and the resulting fragments were cloned into plasmid pECD794 (pLO2-*lacZ*).[17] The respective

operon fusion cassettes were inserted into the open-reading frame of the target gene by conjugation and single cross-over recombination.

Fluorescence assay and *gfp*-reporter plasmid constructions

C. metallidurans cells with a *gfp* reporter gene promoter fusion plasmid were cultivated as a pre-culture in TMM containing 1.5 mg L^{-1} kanamycin at 30 °C. Cultures were shaken at 250 rpm for 30 h, then diluted into fresh medium to a density of 30 Klett units and incubated further at 30 °C. At a cell density of 60 to 70 Klett units, metal salts or EDTA were added to different final concentrations and cells were incubated with shaking for 18 h at 30 °C in a neoLab Shaker DTS-2 (neoLab, Heidelberg, Germany).

The specific GFP fluorescence was calculated as nmol μg^{-1} (dry weight) by using an extinction coefficient (EGFP) at 488 nm of ε = 42 000 l mol^{-1} cm^{-1}, with a layer thickness of the well and coefficient of culture volume to the volume of the reaction mixture. Measurement of the emission wavelength at 518 nm was performed after excitation at 488 nm and the optical density at 600 nm was also measured using a TECAN infinite 200 PRO reader (TECAN, Männersdorf, Switzerland). The dry weight per volume was calculated from the turbidity measurements, using a calibration curve.

The *gfp* reporter gene was amplified (primer: GFP13 KpnI – 5′ AAAGGTACC-ATACATATGGCTAGCAAAG 3′ and GFP13 NsiI 5′ TTAATGCAT-AGTGCTCGAATTCATTATTT 3′) from source Plasmid pMUTIN-GFP+[73] and inserted into pBBR1-MSC2[74] after digestion (NsiI/KpnI) to construct the reporter plasmid. A 100–150 bp PCR-product of the promotor region of the genes (Rmet_2621 *zupT* & Rmet_1098/$cobW_1$) was amplified from total DNA of strain CH34 or AE104 (primer: *zupT*p HindIII – 5′ AAAAAGCTT-CTGCGCTGGCCGCTTCTTC 3′ and *zupT*p KpnI – 5′ AAAGGTACC-CGATTAACGCAACAATGTTGC 3′/$cobW_1$p KpnI – 5′ AAAGGTACC-GGATTTGGTTTGCCCGCAAG 3′ and $cobW_1$p SpeI – 5′ AAAACTAGT-TTCAGGCGACGCAGATAGAC 3′) and the resulting fragments were cloned after digestion (KpnI & SpeI) into plasmid pBBR1-MSC2Φgfp+. The *zupT* promoter region had to be subcloned into the pGEM T-easy (Promega) prior to subsequent subcloning.

Activity stain for membrane-bound hydrogenases

Hydrogen-dependent activities of hydrogenases were visualized by chromogenic detection in non-denaturing polyacrylamide gel electrophoresis (PAGE) using 7.5% (w/v) polyacrylamide, pH 8.5 included 0.1% (w/v) Triton X-100 in the gels. Cell debris, soluble extracts and/or membrane fractions were dissolved in 50 mM Tris-HCl pH 8.0; 150 mM NaCl buffer. Samples (50 μg of protein) were incubated with 4% (w/v) Triton X-100 prior to application to the gels. Hydrogenase activity staining was done as described in Ballantine and Boxer[22] except that the buffer used was 50 mM MOPS pH 7.0, 0.5 mM BV (benzyl viologen) and 1 mM TTC (2,3,5-triphenyltetrazolium chloride) and under anaerobic conditions at RT.

Determination of total hydrogenase enzyme activity

Hydrogenase enzyme activity (H_2-dependent reduction of benzyl viologen) determines the activities of hydrogenases and was measured according to Ballantine and Boxer[22] except that the buffer used was 50 mM MOPS, pH 7.0. No detergent was added to extracts measured by this method. In order to measure hydrogenase activity in solution a wavelength of 578 nm was used, and a molar extinction coefficient value of 8600 M^{-1} cm^{-1} was assumed for reduced benzyl viologen (BV). One unit of activity corresponded to the reduction of 1 μmol of hydrogen per min. Experiments were performed minimally two times and each time in duplicate. Data are presented as standard deviation of the mean.[75]

Enzyme assays with purified proteins

NAD^+ reduction catalyzed by the soluble hydrogenase was measured photometrically as outlined.[76] The method of Schink and Schlegel (1979) was used for the photometric determination of methylene blue reduction catalyzed by the membrane-bound hydrogenase,[77] but glucose, glucose-oxidase, and catalase were omitted. Anaerobic conditions were established by flushing the cuvette, sealed with a rubber stopper, for 10 min with oxygen-free hydrogen. The activity of ribulosebisphosphate carboxylase was assayed radiometrically,[78] the activity of the phosphoribulokinase either radiometrically or photometrically.[79] Protein was determined by the method of Bradford.[80]

Electrophoretic methods

Polyacrylamide gel electrophoresis was performed in a vertical slab gel apparatus (Pantaphor, Fa. Müller, Hann. Münden, Germany) with gels of various concentration and TRIS borate buffer (pH 8.9 or 7.9) as described.[81] To stain gels for hydrogenase activity,[82] the gels were incubated between 1 and 3 h at 30 °C in the dark under a hydrogen atmosphere in 200 mL of 50 mM potassium phosphate buffer, pH 8.0, containing 12 mg 4-nitrobluetetrazolium chloride, 9 mg phenazine methosulfate and, in the case of staining the soluble hydrogenase, 200 μmol of NAD^+. Protein was stained with Coomassie brilliant blue.[83] Sodium dodecylsulfate polyacrylamidgel electrophoresis (SDS-PAGE) was performed in the same apparatus using various polyacrylamide concentrations as described.[84] Electrophoresis was carried out in 100 mM sodium phosphate buffer, pH 7.2, containing 2% SDS. Samples were prepared as follows: solutions of 1 mg protein per mL in 10 mM sodium phosphate buffer, pH 7.2, were incubated with 2% (w/v) SDS and 5% (v/v) 2-mercaptoethanol for 3 min at 100 °C. Cytochrome *c*, chymotrypsinogen, ovalbumin, bovine serum albumin, aldolase, catalase and ferritin were used as molecular mass standards.

Determination of the molecular mass

The relative molecular masses of the enzymes were determined by gel filtration on a Sephacryl S300 column.[85] The same proteins as mentioned above were used as standard proteins. The relative molecular masses were also determined by sucrose gradient centrifugation.[86] A linear sucrose density gradient (5 to 30% sucrose in 50 mM potassium phosphate buffer, pH 7.0) of 11 mL volume was used. The experiment was performed at 30 000 rpm and 4 °C for 28 h in a swing-out rotor and an

OmegalI-ultracentrifuge (Christ, Osterode, Germany). Catalase and lactate-dehydrogenase were used as standard proteins.

Purification procedures

One aim of this work was to purify all of the four key enzymes of the autotrophic metabolism from one cell suspension. Therefore, the purification procedures had steps in common. All purifications involved affinity chromatography using Procion-dye sepharose. The Procion dyes were coupled to Sepharose 4B following the procedure of Atkinson *et al.*[87] They were a gift from the German ICI (Frankfurt).

To prepare the crude extract, the cells were suspended in buffer A (20 mM imidazole-HCI buffer containing 10 mM $MgCl_2$ and 500 μM dithioerythrol) to a final volume of 3 mL per g wet weight. 1 mg DNAse per mL of cell suspension was added, then the suspension was passaged twice through a French press (American Instruments Inc., Silver Springs, Maryland, USA) at 1560 kPa cm^{-2} and the mixture was subsequently centrifuged (10 min 20 000 rpm, Zeta 20, Christ) at 4 °C to remove unbroken cells and cell debris. The resulting cell-free extract was referred to as crude extract for the soluble enzymes, and was centrifuged for 1 h at 35 000 rpm in an Omicron ultracentrifuge (Christ). The sediment was used for the preparation of the membrane-bound hydrogenase, the supernatant for the three soluble enzymes, the soluble hydrogenase, the ribulose bisphosphate carboxylase and the phosphoribulokinase.

To purify the membrane-bound hydrogenase, the sediment from the ultracentrifugation step was re-suspended in 20 mM potassium phosphate buffer (KP20), pH 7.0, containing 0.086 g sucrose per mL and 0.031 mL sodium chloride solution (5 M) per mL suspension, stirred for 15 min at 23 °C and sedimented in the ultracentrifuge (conditions as above). The second sediment also was re-suspended in KP20, pH 7.0, to a final volume of 1 mL per 200 mg membranes. Per mL, 0.1 g sucrose and 0.05 mL solubilization mixture[77] (100 mL L^{-1} Triton X-100, 20 g L^{-1} sodium deoxycholate, 200 mM EDTA) were added. The solution was carefully stirred at room temperature for 30 min and centrifuged (10 min at 20 000 rpm, Zeta 20). This solution was applied onto a column of Procion-Blue HERD-sepharose matrix equilibrated with KP20, pH 7.0, and washed with the same buffer. The hydrogenase was eluted with 1 M KCI in KP20, pH 7.0. Fractions with high hydrogenase activity were combined, concentrated by ultrafiltration in a diaflow chamber (Amicon Corp., USA) using a PM10 filter and layered on the top of a Sephacryl S300 column. KP20, pH 8.0, was used for pre-equilibration and for elution. The most active fractions were combined, concentrated by ultrafiltration as above and applied onto a column of DEAE-Sephacel. This latter column was washed with KP20, pH 8.0, and eluted with a linear gradient of 0 to 1 M KCl in the same buffer.

As common steps for the soluble enzymes, 0.03 mg protamine sulfate were dissolved in 2 mL buffer A per mg of total protein in the supernatant of the first ultracentrifugation step. This solution was added drop-wise with stirring to the supernatant, and stirring was continued for 20 min. The resulting precipitate was removed by centrifugation (20 min 20 000 rpm, Zeta 20). The supernatant was fractionated by addition of pulverized $(NH_4)_2SO_4$ to give a 25% (w/v) saturated solution. After centrifugation (10 min 15 000 rpm, Zeta 20) the precipitate was discarded. Then the supernatant solution was brought to 40% (w/v) saturation of ammonium sulfate and again centrifuged. The pellet contained the CO_2-fixing enzymes, the supernatant the soluble hydrogenase.

For purification of the soluble hydrogenase, this supernatant was brought to 60% (w/v) saturation of $(NH_4)_2SO_4$ and centrifuged. The supernatant was discarded, the sediment dissolved in KP20, pH 7.0, and the conductivity of the final solution adjusted to that of 100 mM KCl in the same buffer. This solution was applied onto a DEAE-Sephacel column. The column was washed with KP20, pH 7.0, and eluted with a linear gradient (0–300 mM KCl) in the same buffer. The most active fractions were combined, concentrated by ultrafiltration as described above and layered on the top of a Sephacryl S300 column. KP20, pH 6.2, was used for pre-equilibration and for elution. The active fractions were combined, concentrated by ultrafiltration and applied onto a Procion-Yellow HE6g column. This last column was washed with KP20, pH 6.2, and eluted with KP20, pH 7.0, containing 50 mM KCl.

The sediment of the second ammonium sulfate precipitation containing the ribulose 1,5-bisphosphate carboxylase and phosphoribulokinase was dissolved in buffer A. It was layered on top of a Sephacryl S300 column, buffer A was used for pre-equilibration and for elution. The fractions within a broad range of activity were collected, concentrated by ultrafiltration and applied onto a Procion-Red HE7b-sepharose column. The column was washed with buffer A and eluted with the same buffer containing 1 M KCl. The active fractions were collected, concentrated by ultrafiltration and again layered on top of a Sephacryl S300 column, which was also pre-equilibrated and eluted with buffer A to separate both enzymes. The most active fractions of both enzymes were collected and concentrated by ultrafiltration.

Aut-negative mutants

Mutants were generated from strain AE104 that were no longer able to grow autotrophically in SGK medium. To isolate the mutants, strain AE104 was treated with the mutagenic agents nitrite, EMS (ethyl-methansulfonate), NMG (*N*-methyl-*N*′-nitro-*N*-nitroso-guanidine), or mitomycin C. For treatment with nitrite, a volume of 5 mL of an overnight NB (nutrient broth) culture were harvested by centrifugation, washed in 5 mL 0.1 M sodium acetate buffer, pH 4.6, and suspended in 1 mL of the same buffer. Solid $NaNO_2$ was added to a final concentration of 50 mM. The cells were incubated 10 min at 30 °C, then 9 mL SGK medium were added. The cells were sedimented by low-spin centrifugation and re-suspended in 1 mL SGK. About 0.5×10^6 of the cells survived this treatment. For EMS mutagenesis, 2.5 mL of an overnight NB culture were added to 2.5 mL EMS-solution (2.4 mL SGK + 0.1 mL EMS). The solution was shaken for 2 h at 37 °C, then 45 mL SGK were added to stop EMD treatment. For NMG, 10 mL of an overnight NB culture were harvested by centrifugation and re-suspended in 1 mL TMA

(1 L H_2O + 6 g Tris + 5.8 g maleic acid + 1 g $MgSO_4 \cdot 7H_2O$ + 5 mg $Ca(NO_3)_2$). 100 μL NMG-solution (1 g L^{-1}) were added, the cells were incubated for 30 min at 30 °C, sedimented and resuspended in 1 mL SGK. Finally, cells were grown in SGK containing 0.2% (w/v) sodium gluconate and different amounts of mitomycin C in the range of 0.2 to 50 mg L^{-1} were added.

As a negative control, the cells not treated with any mutagenic agents were diluted and plated on SGK-agar containing 50 mg L^{-1} sodium pyruvate to allow heterotrophic growth of small pin-point colonies during incubation under air for 2 d. Subsequent cultivation for 3 d under an atmosphere of 80% (v/v) H_2 + 10% O_2 + 10% CO_2 allowed autotrophic growth of parental cells while mutants ceased to grow and remained as pin-points. A total of 3200 of these small colonies were randomly selected and tested for their ability to grow autotrophically on SGK medium. The cells that had been treated with a mutagenic agent were also diluted and plated onto SGK-agar containing 50 mg L^{-1} sodium pyruvate, and the same procedure was followed. Again, 3200 pin-point colonies were tested. In a third independent experiment, the mutagenized cells were sedimented and resuspended in 1 mL SGK. This cell suspension was used as an inoculum for 19 mL SGK containing 9 g L^{-1} sodium gluconate and 3 g L^{-1} glycerol. The culture was shaken for 2 d at 30 °C, 2.5 mL of the culture were washed twice with SGK and resuspended in 20 mL SGK containing 3 g L^{-1} L-histidine. The culture was incubated 2 d under air following 1.5 d under an atmosphere of 80% (v/v) H_2 + 10% O_2 + 10% CO_2, D-cycloserine was added to a final concentration of 1 g L^{-1} to kill autotrophically growing cells, allowing enrichment of mutants. The incubation under a gas atmosphere of 80% (v/v) H_2 + 10% O_2 + 10% CO_2 was continued for 5 h, the cells were washed twice with SGK and resuspended in 10 mL SGK. This suspension was used for pin-point colony selection as described above.

Characterization of the mutants

The mutant strains were grown in IND medium for 3 d, harvested by centrifugation, and disrupted by ultrasonication (3 min at 12.5 μ in a MSE ultrasonic des integrator MK2). The suspension was centrifuged twice (10 min 15 000 rpm, Zeta 20, and 35 000 rpm, 1 h, Omicron). In the supernatant the specific activity of the soluble hydrogenase, the ribulose 1,5-bisphosphate carboxylase, and the phosphoribulokinase was determined. The membranes were washed twice in KP50, pH 7.0, containing 10 mM $MgCI_2$, dissolved in the same buffer and used for the determination of the activity of the membrane-bound hydrogenase.

Reversion-analysis

The mutant strains were grown overnight in NB, diluted and plated onto NB and SGK agar. The NB-plates were incubated under air, the SGK-plates under ''Knallgas'' conditions (80% (v/v) H_2 + 10% O_2 + 10% CO_2). The spontaneous reversion rate was calculated as the ratio of the cells able to grow autotrophically divided by the total cell number. Treating the cells with the chemical procedure that had originally been used to produce the respective mutant strain also induced reversion, and subsequently the reversion rate was determined.

RNA isolation

C. metallidurans CH34, AE104 and Δ*zupT* cells were cultivated heterotrophically in TMM as described above. For the main culture EDTA or zinc chloride were added. At a cell turbidity of 100 Klett, the cells were rapidly harvested at 4 °C and stored at −80 °C. Total RNA was isolated with RNeasy Mini Kit (Qiagen, Hilden, Germany) according to the manufacturer's instructions. A second DNase treatment with a precipitation step was performed. To exclude experimental artifacts resulting from DNA contaminations, only RNA was used that did not generate products in a PCR reaction with chromosomal primers. RNA concentration was determined photometrically, and RNA quality was checked on formamide gels[88] and measured as RNA integrity number (RIN) on an Agilent 2100 Bioanalyzer (Agilent Technologies, Waldbronn, Germany).

Microarrays of *C. metallidurans*

C. metallidurans parental strain CH34 was cultivated without additions (three repeats). Strain AE104 (three per condition) and Δ*zupT* (two repeats per condition) were either grown for 10 min in the presence of 50 μM EDTA or 10 μM zinc chloride. Moreover, strain AE104 was cultivated with or without 100 μM zinc chloride (added for 10 min at a turbidity of 100 Klett). Isolated and quality-checked RNA were provided to IMGM Laboratories GmbH (Martinsried, Germany) for hybridization with a *C. metallidurans* Agilent Custom GE microarray (8 × 15 K) (Agilent Technologies, Waldbronn, Germany) with a single color (Cy3)-based protocol. Signals were detected using the Agilent DNA microarray Scanner. Software tool Feature Extraction 10.7.3.1. was used for raw data extraction.

In the algorithm used, (i) the mean intensity of the pixels of the surrounding area was subtracted from the mean density of the pixels of the spots to give the signal strength. Its deviation was half of the sum of both intensity deviations. The distance (*D*) value was the distance between spot and background pixel intensities divided by the sum of the deviations. *D* was a more useful value than Student's *t*-test because non-touching deviation bars of two values ($D > 1$) at three repeats always indicates at least a significant (>95%) difference. Signals were further processed if $D > 1$. Subsequently, (ii) the mean values of the biological repeats were calculated plus their deviation and the smallest *D* value. Third, (iii) the values from different spots, positions or oligonucleotides assigned to the same gene were taken to calculate a gene-specific mean value and minimum *D*-value. Finally, (iv) the respective spot signals coming from various growth conditions were compared (*Q*- and *D*-values, respectively).

Microarray data accession number

The microarray data were deposited in the GEO database at Gene Expression Omnibus (http://www.ncbi.nlm.nih.gov/geo/) under accession no. GSE64196.

Conclusions

The *aut* region 1 on CMGI-3, which harbors genes for the soluble hydrogenase of *C. metallidurans*, and *aut* region 2 on

CMGI-2, which harbors the genes encoding the membrane-bound hydrogenase, are silenced under conditions of a disturbed metal ion homeostasis or increased zinc availability. This happens when strain CH34 is confronted with a transition metal mixture or when the plasmid-free strain AE104, devoid of the sophisticated plasmid-encoded metal resistance determinants, is cultivated in a phosphate-poor Tris-buffered medium that does not complex transition metal cations very strongly and allows their rapid metal uptake. Histone-like proteins or sigma factors might be involved in this silencing process. Additionally, a global zinc-dependent regulatory process in *C. metallidurans* might be involved, which also controls metal uptake systems and acts in parallel with the Zur zinc uptake regulator. The presence of a *dksA* gene in the same operon region as *zur* and *cobW2* indicates that an interplay between DksA proteins might be responsible for this global zinc-dependent regulatory process. In a second step, silencing of the genes in *aut* region 1 is reverted in the Δ*zupT* mutant of AE104, which has problems to allocate zinc efficiently to zinc-dependent proteins, or in a sigma factor triple mutant with a high cellular nickel content. Together, these data suggest that the zinc-dependent nickel discrimination proteins HypA and HypB are responsible for the ''un-silencing'' of *aut* region 1, as already discussed in detail elsewhere.[8]

Acknowledgements

Funding for this work was provided by the *Deutsche Forschungsgemeinschaft* (Ni262/10). We thank Grit Schleuder for skillful technical assistance and Gary Sawers for helpful comments.

Notes and references

1 K. J. Waldron, J. C. Rutherford, D. Ford and N. J. Robinson, *Nature*, 2009, **460**, 823–830.
2 S. Tottey, D. R. Harvie and N. J. Robinson, in *Molecular microbiology of heavy metals*, ed. D. H. Nies and S. Silver, Springer-Verlag, Berlin, 2007, vol. 6, pp. 3–36.
3 D. H. Nies, in *Molecular microbiology of heavy metals*, ed. D. H. Nies and S. Silver, Springer-Verlag, Berlin, 2007, vol. 6, pp. 118–142.
4 Z. Ma, P. Chandrangsu, T. C. Helmann, A. Romsang, A. Gaballa and J. D. Helmann, *Mol. Microbiol.*, 2014, **94**, 756–770.
5 K. Helbig, C. Bleuel, G. J. Krauss and D. H. Nies, *J. Bacteriol.*, 2008, **190**, 5431–5438.
6 C. Große, G. Schleuder, C. Schmole and D. H. Nies, *Appl. Environ. Microbiol.*, 2014, **80**, 7071–7078.
7 J. A. Imlay, *J. Biol. Chem.*, 2014, **289**, 28121–28128.
8 M. Herzberg, D. Dobritzsch, S. Helm, S. Baginski and D. H. Nies, *Metallomics*, 2014, **6**, 2157–2165.
9 Y. Li and D. B. Zamble, *Chem. Rev.*, 2009, **109**, 4617–4643.
10 R. P. Hausinger and D. B. Zamble, in *Molecular Microbiology of heavy metals*, ed. D. H. Nies and S. Silver, Springer-Verlag, Berlin, 2007, pp. 287–320.
11 M. Mergeay, D. Nies, H. G. Schlegel, J. Gerits, P. Charles and F. van Gijsegem, *J. Bacteriol.*, 1985, **162**, 328–334.
12 C. Schafer, B. Friedrich and O. Lenz, *Appl. Environ. Microbiol.*, 2013, **79**, 5137–5145.
13 M. Bernhard, T. Buhrke, B. Bleijlevens, A. L. De Lacey, V. M. Fernandez, S. P. J. Albracht and B. Friedrich, *J. Biol. Chem.*, 2001, **276**, 15592–15597.
14 P. J. Janssen, R. Van Houdt, H. Moors, P. Monsieurs, N. Morin, A. Michaux, M. A. Benotmane, N. Leys, T. Vallaeys, A. Lapidus, S. Monchy, C. Medigue, S. Taghavi, S. McCorkle, J. Dunn, D. van der Lelie and M. Mergeay, *PLoS One*, 2010, **5**, e10433.
15 A. Kirsten, M. Herzberg, A. Voigt, J. Seravalli, G. Grass, J. Scherer and D. H. Nies, *J. Bacteriol.*, 2011, **193**, 4652–4663.
16 D. H. Nies, *FEMS Microbiol. Rev.*, 2003, **27**, 313–339.
17 J. Scherer and D. H. Nies, *Mol. Microbiol.*, 2009, **73**, 601–621.
18 T. von Rozycki and D. H. Nies, *Antonie van Leeuwenhoek*, 2009, **96**, 115–139.
19 T. von Rozycki, D. H. Nies and M. H. J. Saier, *Comp. Funct. Genomics*, 2005, **6**, 17–56.
20 M. H. J. Saier, C. V. Tran and R. D. Barabote, *Nucleic Acids Res.*, 2006, **34**, D181–D186.
21 M. Herzberg, L. Bauer and D. H. Nies, *Metallomics*, 2014, **6**, 421–436.
22 S. P. Ballantine and D. H. Boxer, *J. Bacteriol.*, 1985, **163**, 454–459.
23 I. H. Segel, *Enzyme kinetics*, John Wiley and Sons, New York, 1975.
24 S. Frielingsdorf, J. Fritsch, A. Schmidt, M. Hammer, J. Lowenstein, E. Siebert, V. Pelmenschikov, T. Jaenicke, J. Kalms, Y. Rippers, F. Lendzian, I. Zebger, C. Teutloff, M. Kaupp, R. Bittl, P. Hildebrandt, B. Friedrich, O. Lenz and P. Scheerer, *Nat. Chem. Biol.*, 2014, **10**, U378–U392.
25 J. Fritsch, P. Scheerer, S. Frielingsdorf, S. Kroschinsky, B. Friedrich, O. Lenz and C. M. T. Spahn, *Nature*, 2011, **479**, 249–252.
26 A. Toussaint, C. Merlin, S. Monchy, M. A. Benotmane, R. Leplae, M. Mergeay and D. Springael, *Appl. Environ. Microbiol.*, 2003, **69**, 4837–4845.
27 R. Van Houdt, S. Monchy, N. Leys and M. Mergeay, *Antonie van Leeuwenhoek*, 2009, **96**, 205–226.
28 R. Antoine, F. Jacob-Dubuisson, H. Drobecq, E. Willery, S. Lesjean and C. Locht, *J. Bacteriol.*, 2003, **185**, 1470–1474.
29 Y. Taniguchi, P. J. Choi, G.-W. Li, H. Chen, M. Babu, J. Hearn, A. Emili and X. S. Xie, *Science*, 2010, **329**, 533–538.
30 M. L. Coleman, M. B. Sullivan, A. C. Martiny, C. Steglich, K. Barry, E. F. DeLong and S. W. Chisholm, *Science*, 2006, **311**, 1768–1770.
31 M. Gaillard, T. Vallaeys, F. J. Vorholter, M. Minoia, C. Werlen, V. Sentchilo, A. Puhler and J. R. van der Meer, *J. Bacteriol.*, 2006, **188**, 1999–2013.
32 J. E. Peters, A. D. Fricker, B. J. Kapili and M. T. Petassi, *Mol. Microbiol.*, 2014, **93**, 1084–1092.
33 C. Dressler, U. Kües, D. H. Nies and B. Friedrich, *Appl. Environ. Microbiol.*, 1991, **57**, 3079–3085.

34 S. Kar, R. Edgar and S. Adhya, *Proc. Natl. Acad. Sci. U. S. A.*, 2005, **102**, 16397–16402.
35 M. Macvanin and S. Adhya, *Biochim. Biophys. Acta, Gene Regul. Mech.*, 2012, **1819**, 830–835.
36 M. Macvanin, R. Edgar, F. Cui, A. Trostel, V. Zhurkin and S. Adhya, *J. Bacteriol.*, 2012, **194**, 6046–6055.
37 J. Oberto, S. Nabti, V. Jooste, H. Mignot and J. Rouviere-Yaniv, *PLoS One*, 2009, **4**, e4367.
38 A. Balandina, L. Claret, R. Hengge-Aronis and J. Rouviere-Yaniv, *Mol. Microbiol.*, 2001, **39**, 1069–1079.
39 A. Kuroda, K. Nomura, N. Takiguchi, J. Kato and H. Ohtake, *Cell. Mol. Biol.*, 2006, **52**, 23–29.
40 A. Ishihama, A. Kori, E. Koshio, K. Yamada, H. Meada, T. Shimada, H. Makinoshima, A. Iwata and N. Fujita, *J. Bacteriol.*, 2014, **196**, 2718–2727.
41 W. W. Navarre, S. Porwollik, Y. P. Wang, M. McClelland, H. Rosen, S. J. Libby and F. C. Fang, *Science*, 2006, **313**, 236–238.
42 S. T. Arold, P. G. Leonard, G. N. Parkinson and J. E. Ladbury, *Proc. Natl. Acad. Sci. U. S. A.*, 2010, **107**, 15728–15732.
43 J. D. Helmann, *Adv. Microb. Phys.*, 2002, **46**, 47–110.
44 M. A. Lonetto, K. L. Brown, K. E. Rudd and M. J. Buttner, *Proc. Natl. Acad. Sci. U. S. A.*, 1994, **91**, 7573–7577.
45 C. Große, S. Friedrich and D. H. Nies, *J. Mol. Microbiol. Biotechnol.*, 2007, **12**, 227–240.
46 D. H. Nies, *Arch. Microbiol.*, 2004, **181**, 255–268.
47 D. H. Nies, G. Rehbein, T. Hoffmann, C. Baumann and C. Grosse, *J. Mol. Microbiol. Biotechnol.*, 2006, **11**, 82–93.
48 C. Tibazarwa, S. Wuertz, M. Mergeay, L. Wyns and D. van der Lelie, *J. Bacteriol.*, 2000, **182**, 1399–1409.
49 G. Grass, B. Fricke and D. H. Nies, *BioMetals*, 2005, **18**, 437–448.
50 G. Grass, C. Große and D. H. Nies, *J. Bacteriol.*, 2000, **182**, 1390–1398.
51 S. Leonhartsberger, A. Huber, F. Lottspeich and A. Böck, *J. Mol. Biol.*, 2001, **307**, 93–105.
52 R. C. Weast, *CRC handbook of chemistry and physics*, CRC Press, Inc., Boca Raton, Florida, USA, 64th edn, 1984.
53 H. G. Schlegel, G. Gottschalk and H. Kaltwasser, *Arch. Microbiol.*, 1961, **38**, 209–222.
54 R. M. C. Dawson, D. C. Elliott, W. H. Elliott and K. M. Jones, *Data for biochemical research*, Clarendon Press, Oxford, 2nd edn, 1969.
55 R. J. Jackson, M. R. B. Binet, L. J. Lee, R. Ma, A. I. Graham, C. W. McLeod and R. K. Poole, *FEMS Microbiol. Lett.*, 2008, **289**, 219–224.
56 S. McCarthy, C. Ai, G. Wheaton, R. Tevatia, V. Eckrich, R. Kelly and P. Blum, *J. Bacteriol.*, 2014, **196**, 3562–3570.
57 C. Schmidt, C. Schwarzenberger, C. Grosse and D. H. Nies, *J. Bacteriol.*, 2014, **196**, 3461–3471.
58 M. Napolitano, M. A. Rubio, J. Santamaria-Gomez, E. Olmedo-Verd, N. J. Robinson and I. Luque, *J. Bacteriol.*, 2012, **194**, 2426–2436.
59 B. Thony, G. Auerbach and N. Blau, *Biochem. J.*, 2000, **347**, 1–16.
60 D. C. Brown and K. D. Collins, *J. Biol. Chem.*, 1991, **266**, 1597–1604.
61 C. M. Zhang, T. Christian, K. J. Newberry, J. J. Perona and Y. M. Hou, *J. Mol. Biol.*, 2003, **327**, 911–917.
62 G. Auerbach, A. Herrmann, A. Bracher, G. Bader, M. Gutlich, M. Fischer, M. Neukamm, M. Garrido-Franco, J. Richardson, H. Nar, R. Huber and A. Bacher, *Proc. Natl. Acad. Sci. U. S. A.*, 2000, **97**, 13567–13572.
63 C. M. Zhang, J. J. Perona and Y. M. Hou, *Biochemistry*, 2003, **42**, 10931–10937.
64 C. E. Blaby-Haas, J. A. Flood, V. de Crecy-Lagard and D. B. Zamble, *Metallomics*, 2012, **4**, 488–497.
65 C. E. Haas, D. A. Rodionov, J. Kropat, D. Malasarn, S. S. Merchant and V. de Crecy-Lagard, *BMC Genomics*, 2009, **10**, 1–21.
66 P. Chandrangsu, J. J. Lemke and R. L. Gourse, *Mol. Microbiol.*, 2011, **80**, 1337–1348.
67 A. Perederina, V. Svetlov, M. N. Vassylyeva, T. H. Tahirov, S. Yokoyama, I. Artsimovitch and D. G. Vassylyev, *Cell*, 2004, **118**, 297–309.
68 M. N. Vassylyeva, A. A. Perederina, V. Svetlov, S. Yokoyama, I. Artsimovitch and D. G. Vassylyev, *Acta Crystallogr., Sect. D: Biol. Crystallogr.*, 2004, **60**, 1611–1613.
69 N. Pfennig, *Arch. Microbiol.*, 1974, **100**, 197–206.
70 C. N. Pace and M. J. Scholtz, in *Protein structure: a practical approach*, ed. T. Creighton, IRL press, Oxford, UK, 1997, pp. 299–322.
71 A. Anton, A. Weltrowski, J. H. Haney, S. Franke, G. Grass, C. Rensing and D. H. Nies, *J. Bacteriol.*, 2004, **186**, 7499–7507.
72 D. H. Nies, *J. Bacteriol.*, 1992, **174**, 8102–8110.
73 M. Kaltwasser, T. Wiegert and W. Schumann, *Appl. Environ. Microbiol.*, 2002, **68**, 2624–2628.
74 M. E. Kovach, P. H. Elzer, D. S. Hill, G. T. Robertson, M. A. Farris, R. M. Roop, 2nd and K. M. Peterson, *Gene*, 1995, **166**, 175–176.
75 C. Pinske, S. Kruger, B. Soboh, C. Ihling, M. Kuhns, M. Braussemann, M. Jaroschinsky, C. Sauer, F. Sargent, A. Sinz and R. G. Sawers, *Arch. Microbiol.*, 2011, **193**, 893–903.
76 K. Schneider and H. G. Schlegel, *Biochim. Biophys. Acta*, 1976, **452**, 66–80.
77 B. Schink and H. G. Schlegel, *Biochim. Biophys. Acta*, 1979, **567**, 315–324.
78 B. Bowien, F. Mayer, G. A. Codd and H. G. Schlegel, *Arch. Microbiol.*, 1976, **110**, 157–166.
79 K. Siebert, P. Schobert and B. Bowien, *Biochim. Biophys. Acta*, 1981, **658**, 35–44.
80 M. M. Bradford, *Anal. Biochem.*, 1976, **72**, 248–254.
81 H. Stegemann, H. Francksen and V. Macko, *Z. Naturforsch.*, 1973, **28C**, 722–732.
82 M. Pinkwart, K. Schneider and H. G. Schlegel, *Biochim. Biophys. Acta*, 1983, **745**, 262–278.
83 K. Weber and M. Osborn, *J. Biol. Chem.*, 1969, **244**, 4406–4412.
84 K. Weber, J. R. Pringle and M. Osborn, *Methods Enzymol.*, 1972, **26**, 3–27.

85 P. Andrews, *Biochem. J.*, 1964, **91**, 222–233.
86 R. G. Martin and B. N. Ames, *J. Biol. Chem.*, 1961, **236**, 1372–1379.
87 T. Atkinson, P. M. Hammond, R. D. Hartwell, P. Hughes, M. D. Scawen, R. F. Sherwood, D. A. P. Small, C. J. Bruton, M. I. Harvey and C. R. Lowe, *Biochem. Soc. Trans.*, 1981, **9**, 290–293.
88 J. Sambrook, E. F. Fritsch and T. Maniatis, *Molecular cloning, a laboratory manual*, Cold Spring Harbor Laboratory, Cold Spring Harbor, N.Y., 2nd edn, 1989.